Current Radiopharmaceuticals, 2020, *13*, 63-79

REVIEW ARTICLE

Toward the Discovery and Development of PSMA Targeted Inhibitors for Nuclear Medicine Applications

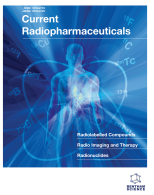

Sara Pastorino[1], Mattia Riondato[1], Licia Uccelli[2,3], Giampiero Giovacchini[1], Elisabetta Giovannini[1], Valerio Duce[1] and Andrea Ciarmiello[1,*]

[1]*Nuclear Medicine Department, S. Andrea Hospital, Via Vittorio Veneto 197, 19124 La Spezia, Italy;* [2]*Morphology, Surgery and Experimental Medicine Department, University of Ferrara, Via L. Borsari 46, 44121 Ferrara, Italy;* [3]*Nuclear Medicine Unit, University Hospital, Via Aldo Moro 8, 44124 Ferrara, Italy*

Abstract: ***Background*:** The rising incidence rate of prostate cancer (PCa) has promoted the development of new diagnostic and therapeutic radiopharmaceuticals during the last decades. Promising improvements have been achieved in clinical practice using prostate specific membrane antigen (PSMA) labeled agents, including specific antibodies and small molecular weight inhibitors. Focusing on molecular docking studies, this review aims to highlight the progress in the design of PSMA targeted agents for a potential use in nuclear medicine.

Results: Although the first development of radiopharmaceuticals able to specifically recognize PSMA was exclusively oriented to macromolecule protein structure such as radiolabeled monoclonal antibodies and derivatives, the isolation of the crystal structure of PSMA served as the trigger for the synthesis and the further evaluation of a variety of low molecular weight inhibitors. Among the nuclear imaging probes and radiotherapeutics that have been developed and tested till today, labeled Glutamate-ureido inhibitors are the most prevalent PSMA-targeting agents for nuclear medicine applications.

Conclusion: PSMA represents for researchers the most attractive target for the detection and treatment of patients affected by PCa using nuclear medicine modalities. [^{99m}Tc]MIP-1404 is considered the tracer of choice for SPECT imaging and [^{68}Ga]PSMA-11 is the leading diagnostic for PET imaging by general consensus. [^{18}F]DCFPyL and [^{18}F]PSMA-1007 are clearly the emerging PET PSMA candidates for their great potential for a widespread commercial distribution. After paving the way with new imaging tools, academic and industrial R&Ds are now focusing on the development of PSMA inhibitors labeled with alpha or beta minus emitters for a theragnostic application.

ARTICLE HISTORY

Received: May 23, 2019
Revised: July 15, 2019
Accepted: July 15, 2019

DOI:
10.2174/1874471012666190729151540

Keywords: Prostate cancer, PSMA, molecular docking, PET, SPECT, imaging, radionuclide therapy.

1. INTRODUCTION

Prostate cancer is the second cause of cancer death and the most frequently diagnosed cancer among males, with almost 1,3 million new cases per year worldwide [1]. Despite the 359,000 associated deaths in 2018, PCa mortality has been decreasing in many developed countries, mostly attributed to the widespread use of prostate-specific antigen (PSA) blood testing [2].

PSA has been revolutionizing PCa screening since it is recognized to be effective in the detection of recurrent disease after primary curative treatment such as Radical Prostatectomy (RP) or local definitive Radiotherapy (RT). This disease state, also defined as Biochemical Recurrence (BCR), is characterized by rising PSA levels after initial curative treatment of PCa [3].

Beside the clinical relevance, PSA screening is still debated because the number of new diagnoses as a result of screening is not always correlated with the extent of the disease and PCa mortality rate. Furthermore, other dysfunctions such as benign prostatic hyperplasia, prostatitis, inflammation or other conditions may lead to high serum PSA levels [4, 5].

During the last decades, new diagnostic/prognostic tools have been introduced in clinical practice to best support the management of prostate cancer patients and in order to overcome PSA measurement constraints.

Multiparametric Prostate Magnetic Resonance (MRI) remains the imaging modality of choice in this context for detecting, characterizing and staging the extent of disease. However, the use of nuclear imaging modalities associated

*Address correspondence to this author at the Nuclear Medicine Department, S. Andrea Hospital, 19124, La Spezia, Italy; Tel: 0187533011; E-mail: andrea.ciarmiello@asl5.liguria.it

1874-4729/20 $65.00+.00

with the use of radiopharmaceuticals, gained a relevant role during the last years for the evaluation of urogenital diseases with a particular address for PCa.

The availability of new tools to aid in the diagnosis and classification of the disease stage is certainly of utmost importance for monitoring the recurrence and evaluating the treatment success over the disease [2]. Taking advantage from the continuous scientific discoveries and technical improvements novel biochemical pathways have been studied by researchers, as well as cell structures potentially relevant as targets for the disease treatment. Among these, the prostate-specific membrane antigen is continuously increasing in importance as "platform" for the development of specific agents for both pharmaceutical and radiopharmaceutical applications.

This review proposes to highlight the progress in the design of PSMA targeted agents for potential use in nuclear medicine over 20 years, from the endogenous substrate of the enzyme up to the radiopharmaceuticals which reached clinical trial setting for PCa imaging and therapy.

Making a comparison with the parallel research in pharmaceutical R&D and focusing on molecular docking studies, this work is aimed to elucidate the structural features responsible to improve both binding and pharmacokinetic properties, which permitted to develop the most promising agents.

2. METHODS

A literature research of studies on prostate cancer, GCPII crystal structure and PSMA inhibitors used in PCa imaging and therapy, was carried out in the period 1995-2019. PubMed, SciFinder, and ScienceDirect databases were consulted for this purpose. Boolean search criteria included the following terms: prostate cancer, PSMA, PET, SPECT, imaging, therapy. RCSB protein data bank (PDB) and UCFS Chimera were also used for studies of molecular docking on the crystal structure of PSMA. American and European CT databases, ClinicalTrials.gov and Clinicaltrialregister.eu were consulted in order to identify radiopharmaceuticals currently tested in clinical studies.

3. ESTABLISHED AND EMERGING NUCLEAR MEDICINE MODALITIES FOR THE PROSTATE CANCER: THE CENTRAL ROLE OF PSMA

Current clinical imaging modalities include transrectal ultrasonography (TRUS), used for biopsy guidance and brachytherapy seed placement, magnetic resonance imaging (MRI) and computed tomography (CT) for PCa staging and metastatic spread detection and bone scintigraphy for the evaluation of bone metastases. These traditional imaging techniques suffer from poor sensitivity and specificity for the detection of early/subtle recurrence or metastasis, *e.g*., lymph nodes and sclerotic bone metastases [6].

More recently, Positron Emission Tomography (PET/CT) has gained a significant role in diagnostic imaging of PCa. Since [^{18}F]fluoro-deoxyglucose ([^{18}F]FDG), the most widely employed radiotracer, has been proved suboptimal in PCa diagnosis because of the relatively low glycolytic rate of the disease [7], other agents have been investigated and later introduced in the daily nuclear medicine practice.

The most effective PET radiopharmaceuticals in this clinical context have been demonstrated to be choline derivatives, in particular [^{11}C]choline and [^{18}F]fluoromethylcholine, which rationale of use is based on the increased phospholipid metabolism in proliferating cancer cells [8]. For the detection of primary prostate cancer, [^{11}C]choline takes advantage of the lower urinary excretion, which favors the observation at the prostatic lodge level. On the other hand, its use is affected by the short half-life (20 min) [9] and the limited production and use by cyclotron-based facilities. In addition, an undesired overlap with the uptake in prostatitis or benign prostatic hypertrophy has been observed [10]. Conversely [^{18}F]fluoromethylcholine, allows a more comfortable procedure in a large number of PET centers, due to the favorable half-life of 110 min. Unfortunately [^{18}F]fluoromethylcholine has a higher urinary excretion than [^{11}C]choline, which makes more difficult the diagnosis of local relapse [9].

The emerging tracer [^{18}F]fluciclovine, a synthetic amino acid which targets overexpressed multiple sodium-dependent and independent channels, seems to outperform labeled choline derivatives in clinical settings. Favorable emitting properties of fluorine-18 and the minimized urinary excretion facilitate the evaluation of the prostate bed and surrounding structures including bladder and urethra, making this novel radiotracer a valuable tool [11]. However, further investigation is warranted to validate these recent results and until now, [^{18}F]fluoromethylcholine and [^{11}C]choline remain the gold standard in PET/CT for patients with recurrent PCa, due to the widespread clinical use and the large available literature.

Their established use also confirmed some heavy limitations of the method, such the relatively poor sensitivity and specificity, especially at low PSA levels and high Gleason scores [12], making the development of alternative diagnostic agents an attractive challenge for radiochemists and radiopharmacists.

More specific markers for the disease than metabolic hallmark, including cell surface proteins, glycoprotein, receptors, enzymes and peptides, have therefore received increased attention during the past years.

Among a large number of candidates, prostate-specific membrane antigen (PSMA) has been studied for more than two decades as a model for the development of PCa diagnostic and therapeutic agents.

PSMA, also known as folate hydrolase I (FOLH1) and glutamate carboxypeptidase II (GCPII), is a 750-aminoacide type II transmembrane glycoprotein constitutively expressed in healthy human tissue such as lacrimal and salivary glands, epididymis, ovary, normal human prostate epithelium, astrocytes and Schwann cells in the nervous central system (CNS) and within the brush border of the jejunum in the small intestine [6, 10, 13]. PSMA exhibits two predominant enzymatic activities: the hydrolytic cleavage of γ-linked glutamates from poly-γ-glutamyl folate and the proteolysis of the neuropeptide N-acetyl-L-aspartyl-L-glutamate (NAAG) [10].

The cleavage of folic acid from poly-γ-glutamyl folate in the small intestine, increases the intestinal uptake of folate, while the hydrolysis of NAAG to N-acetyl-L-aspartate

(NAA) and L-glutamate, modulates neuron-neuron signal transduction and facilitates communication between neurons and support cells (astrocytes, Schwann cells) [14]. The control of glutamatergic neurotransmission mediated by PSMA inhibition has been proved to be a promising pharmacologic approach for the treatment of stroke, amyotrophic lateral sclerosis, inflammatory and neuropathic pain and other neurological disorders associated with glutamate excitotoxicity [15].

In addition to its enzymatic functions, PSMA is upregulated (1000-fold higher than physiologic levels) [16] and strongly expressed in prostate cancer cells, especially in hormone refractory PCa, and in the lymph nodes, bone, rectum, and lung metastasized tumor tissues [6, 10, 13, 14].

Not least importantly, PSMA is also expressed in the endothelium of tumor-associated neovasculature of multiple non-prostatic solid tumor (transitional cell carcinomas, renal cell carcinomas, colon, oesophageal, thyroid, lung and brain cancer), yet largely absent in the vasculature of healthy tissues [6, 10, 13, 14].

The dual nature of PSMA to act as a tumor marker as well as an enzyme, characterized by an active site in a large extracellular domain, boosted the interest for the development of molecular probes with high affinity and specificity for cancer cell targeting [17].

Two distinct approaches have been used during the last twenty years for targeting PSMA and for the development of new radiotracers. In the beginning, the research was mainly focused on the macromolecular protein structure of PSMA to provide specific monoclonal antibodies directed to an epitope of PSMA.

More recently with the isolation of the crystal structure of PSMA in 2005 [18], a dramatic change in strategy occurred, as the enzymatic activity of PSMA served as the trigger for the synthesis and the further evaluation of a variety of anti-PSMA inhibitors of low molecular weight, with the potential to be used as nuclear imaging probes and therapeutic agent [17].

The latter approach is currently the most dynamic and generally applied with a large number of agents involved in clinical trials although the use of monoclonal antibodies and derivatives has been never abandoned, collecting a long experience of failures and successes and thanks to the more and more sophisticated biological techniques.

4. DEVELOPMENT OF ANTI-PSMA MONOCLONAL ANTIBODIES, ANTIBODIES FRAGMENTS AND APTAMERS

The first PSMA targeted radiotracer to find a clinical application has been [^{111}In]capromab pendetide, better known with trade mark ProstaScint™. Capromab (7E11-C5) is a monoclonal antibody developed by the cell membrane of a human prostate cancer cell line, LNCaP [19], functionalized with the open chelator diethylenetriaminepentaacetic acid (DTPA) and labeled with indium-111 [20].

ProstaScint™ was approved by the Food and Drug Administration (FDA) in 1997 as an imaging agent for PSMA, with the primary indication for use in patients with negative bone scans who are at high risk for metastases [8], mainly pelvic lymph node metastasis [10]. It has also been employed in post-prostatectomy patients with rising PSA and negative or equivocal standard metastatic evaluation in high clinical suspicion of occult metastatic disease [8, 10].

Although ProstaScint™ showed to be useful for the identification of recurrent metastatic prostate cancer not detectable by conventional anatomic imaging [6], its efficacy is hampered by some intrinsic drawbacks that have been limiting its clinical application. 7E11-C5 binds a six amino acid sequence on the intracellular epitope that are exposed upon cell death. As a consequence, capromab can be effective in targeting PSMA only through the disruption of the cell membrane, which typically occurs in states of necrosis and apoptosis. In tissues such as bone, where access to the target is even more limited than in soft tissue, ProstaScint™ has proved unable to reliably detect metastases [10]. In addition [^{111}In]capromab pendetide exhibits a long blood clearance and a marked retention in the liver, kidney, and other non-prostate sites, especially in the lower abdomen and pelvis, which creates background signal that often masks the prostate [10].

Other monoclonal antibodies and antibody derivatives targeting PSMA have been tested as a second generation class of agents with improved kinetic properties beyond ProstaScint™ [6], and among these, J591 has been by far the most widely investigated. This de-immunized monoclonal antibody binds with high affinity to viable cells expressing PSMA on the outside of the cell membrane, overcoming the capromab major constraint [10].

The conjugation with 1,4,7,10-tetraazacyclododecane-1,4,7,10- tetraacetic acid (DOTA), a cyclic chelator suitable for the stabilization of a large variety of radiometals, allowed the use of J591 for both imaging and therapeutic purpose. Functionalized J591 antibody has been successfully radiolabeled with ^{111}In,^{99m}Tc and ^{89}Zr for imaging and with ^{90}Y,^{177}Lu and ^{225}Ac for therapy [21-24].

Unfortunately, similar to ProstaScint™, an undesired uptake in non-target organs (such as liver, kidneys, and spleen which is a common distribution pattern for antibodies) has been observed [22]. Despite the general advancements antibody-mediated imaging confirmed to endure from intrinsically suboptimal pharmacokinetics including poor tumor penetration and slow clearance from normal tissues, that produce significant background radioactivity [25]. Other significant drawbacks are the high cost associated with their production and conjugation with a suitable chelating system, as well as a problematic labeling chemistry [26].

A common strategy to optimize the pharmacokinetics of the monoclonal antibodies is to reduce the overall dimension generating antibody fragments with a maintained affinity for the epitopes, such as minibodies or nanobodies [17]. IAB2M, an 80-kDa minibody genetically engineered from the antibody J591 faced at the clinical status [27]. A phase I dose-escalation study (ClinicalTrials.gov, NCT02349022) with ^{89}Zr-desferrioxamine-IAB2M ([^{89}Zr]IAB2M), in patients with metastatic prostate cancer showed a favorable biodistribution and the ability to target both bone and soft-tissue lesions [28].

Nanobodies contain antibody-derived fragments of 15 kDa (typically the variable domain of heavy chain antibodies) that largely retain the specific antigen binding properties of the original antibodies, but with more rapid pharmacokinetics and lower immunogenic potential [27]. Several nanobodies radiolabeled with ^{99m}Tc have been tested and compared for cell binding as internalization, as well as *in vivo* distribution, on PSMA^{pos} LNCaP and PSMA^{neg} PC3 cell lines and tumor-bearing xenografts [29].

Among these nanobodies, PSMA30 stands out for the specific recognition of cell-expressed PSMA, the efficient internalization, the fast clearance and relatively high uptake in PSMA-positive tumors, thus generating high tumor-to organ ratios [29].

Another strategy for overcoming the general poor pharmacokinetics of antibodies relays in the use of aptamers as PSMA targeting agents [10]. Aptamers are short DNA, RNA or peptide oligomers able to assume a specific and stable three-dimensional shape *in vivo*. They exhibit high affinity and specificity for the target, similar to antibodies, achieved by a three-dimensional conformation complementary to the epitope surface [27]. Consisting of 8-15 kDa weight, aptamers are close in size to peptides (1-5 kDa) and slightly smaller than single-chain variable-fragment antibodies (scFvs, 25 kDa) [30, 31].

Recently, two synthetic RNA aptamers, A9 and A10, able to bind the extracellular portion of PSMA with low nanomolar affinity, have been developed and evaluated as potential specific targeting agents of prostate cancer [32]. The small size and polyanionic nature of aptamers lead to rapid blood clearance and tissue uptake and minimize the persistence in liver and kidney, thus it is believed to provide some potentially useful features for imaging and radiotherapy [31].

5. PSMA INSIGHT: DESIGN OF SMALL-LIGANDS WITH AN AFFINITY FOR THE ENZYMATIC POCKET

Low-molecular-weight ligands have several advantages over antibodies, which are more frequently used for specific cell targeting. Small ligands are generally easy to prepare on a large scale, display favorable pharmacokinetic properties (such as bioavailability, biological half-life, *etc*.), and might also penetrate the blood-brain barrier. A great number of potent (below nanomolar) inhibitors have been developed from the insight of PSMA enzymatic pocket [14].

The isolation of PSMA crystal structure was a crucial discovery, providing an un-precedent understanding of the critical interactions of potent agonists and antagonists within the active site. PSMA belongs to the superfamily of zinc-dependent exopeptidases and it consists of a symmetric dimer with each polypeptide chain containing three domains (Fig. **1A**) a protease domain (residues 56-116 and 352-591), an apical domain (residues 117-351), and a helical domain (residues 592-750). A large cavity at the interface between the three domains contains the dinuclear zinc(II) active site [18]. The two zinc ions, separated by almost 3.2 Å, are each coordinated by three endogenous aminoacidic ligands (Fig. **1B**) the catalytic Zn^{2+} is coordinated by His-553 and Glu-425, while the co-catalytic Zn^{2+} is engaged by His-377 and Asp-453. The Asp-387 side chain bridges both zincs in a bidentate state. The presence of the bridging hydroxide anion is of utmost importance for the PSMA enzymatic properties (at the distance of 1.79 Å and 2.26 Å from the co-catalytic and catalytic zinc, respectively) and the Glu-424 proton shuttle [13, 33].

The substrate binding cavity might be simply described as a funnel-shaped accessory tunnel [6] terminated at the bottom by a bulging pharmacophore pocket (S1' pocket) (Fig. **1C**) [33], but an extensive description is needed to help in understanding the reasons which lead to the design of chemical scaffolds in the development of new PSMA tracers.

The pharmacophore pocket S1' has high affinity for glutamate and glutamate-like chemical moieties, as demonstrated by the known natural GCPII substrates (NAAG and folyl-poly-γ-glutamates), which includes a glutamate as the C-terminal residue. As consequence, many PSMA-specific inhibitors have been developed from the glutamate (or NAAG) scaffolds [13] and the molecule region, which interact with the S1' pocket is conventionally named as P1' group.

The internal cavity can be shielded from the external space by the entrance lid, a flexible loop containing amino acids Trp-541 and Gly-548. Crystallographic studies revealed two major conformations of the entrance lid, defined as open and closed. The transition between the two conformations is enabled by flipping of the peptide bond between Asn-540 and Trp-541 at one hinge, and flexibility of Gly-548 at the other one [33].

In the closed conformation the entrance lid forms a capped precluding communication between the enzyme interior and the external space, thus hampering any interaction with the zinc active site. On the contrary the open conformation is observed in GCPII complexes with inhibitors featuring extended moieties, where the closed conformation would be sterically prohibited due to the interference of bulky inhibitor moieties [33].

The S1 pocket, defined as the "non-pharmacophore pocket", encompasses the whole funnel from its narrow (approximately 8 Å) base at the active-site zinc ions to the funnel rim or entrance lid residues in closed conformation [33-35]. This includes an extended, positively charged surface area termed the "arginine patch", which is a spatial arrangement of three arginines (Arg-463, -534, and -536), clustered within 4.5 Å of each other and located 6-12 Å from the nearest zinc ion [18].

The arginine patch is supported by the presence of a chloride ion that stabilizes the side chain of Arg-534 in an invariant, though energetically unfavorable, 'all-gauche' conformation. Differently the remaining arginine residues are characterized by positional variability, thus becoming an attractive feature for the inhibitor design [33].

The Arg-536 side chain can adopt two distinct conformations referred to as "stacking" in the ligand-free form of the enzyme and "binding" when a ligand (inhibitor or substrate) is bound. The transition between these two states is associated with the Arg-463 side chain switch, defined as "up" and

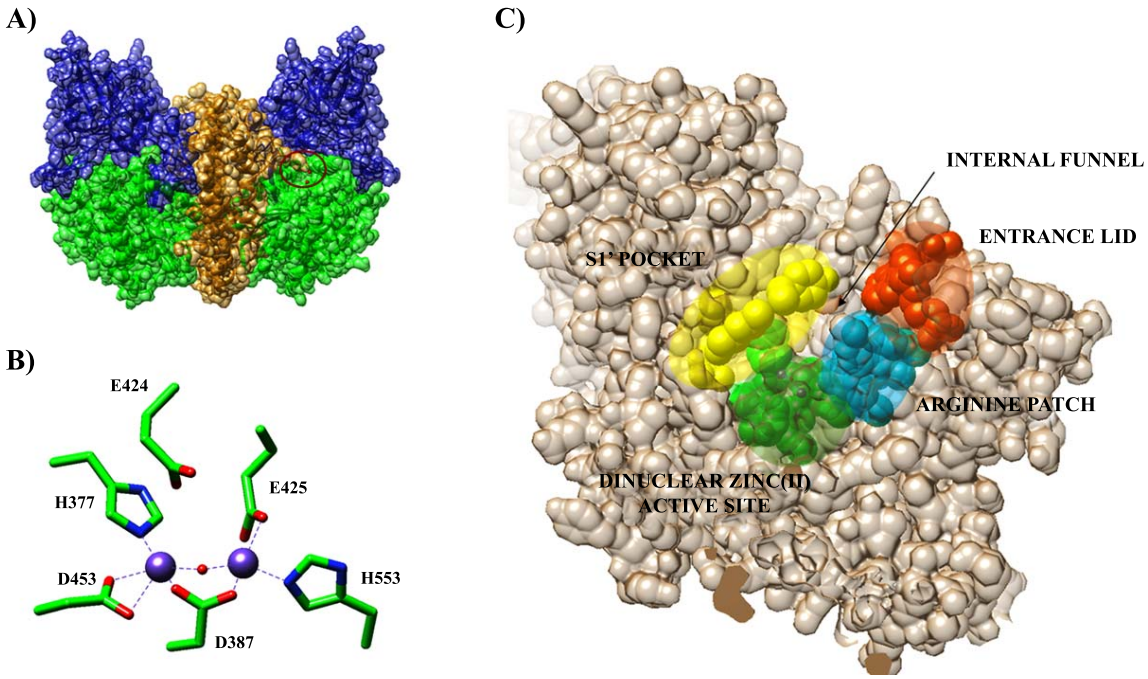

Fig. (1). Crystal structure of human GCPII homodimer. **A**, the surface rendering shows protease domain (green), apical domain (blue), helical domain (yellow) and the active-site zinc ions (red spheres). PSMA active-site is encircled. **B**, interactions of zinc ions (purple spheres) with water (red sphere) and residues lining the active site of PSMA. **C**, internal cavity of human GCPII: surface representation of the S1' pocket (yellow), the active-site (green), the arginine patch (cyan) and the entrance lid (orange) (realized by UCSF Chimera, PDB code 1Z8L).

"down" positions [34]. The binding conformation of Arg-536 and the simultaneous relocation of the Arg-463 side chain form the S1 hydrophobic accessory pocket (previously hidden) of 7 Å x 8.5 Å x 9 Å [33].

The third and last prominent structural feature that can play an important role in interactions with GCPII ligands is the arene-binding site (ABS), a simple structural motif shaped by the side chains of Arg-463, Arg-511, Trp-541 and part of the GCPII entrance lid. The arene-binding site together with the hydrophobic accessory pocket, determines the structural plasticity in the S1 site/entrance funnel of GCPII [35].

With these premises pharmaceutical and radiopharmaceutical R&D addressed their strength many small molecule substrates and inhibitors with high specificity for the enzyme pocket S1'.

In the beginning, efforts regarded extensive structure-activity relationships (SAR), mainly aimed at identifying suitable substitutions of the terminal glutamate that would improve the physicochemical and biologic features of target ligands. However, all such substitutions have failed to provide viable leads and instead have resulted in compounds with substantially lower PSMA affinities.

Consequently, the research of low molecular weight ligand shifted from the modification of glutamate itself to a more comprehensive approach: the development of a suitable zinc binding coordinating motif preserving the glutamate or including a glutamate isostere.

Three families of compounds are herein presented and discussed: (1) phospho(i)nate compounds and thiols; (2) glutamate-phosphoramidates; and (3) glutamate-ureido derivatives (Fig. **2**) [10].

At first, among phospho(i)nate and thiol derivatives, new molecular entities with a PSMA specific interaction were developed by academies and pharmaceutical industry for applications other than nuclear medicine, as a milestone for further advancements.

Glutatamate-phophoramidate and ureido-based PSMA inhibitors have been studied for nuclear medicine application. Among these compounds, the ureido-based inhibitors are currently the most employed PSMA-targeting agents both for imaging and therapeutic applications [36].

Considering the utmost importance of the latter group of compounds, further classification is proposed, guiding the reader among the discovery of the most employed labeled compounds. Among them, special mentions are dedicated to fluorine-18 derivatives and the agents for conventional imaging, as well as for gallium-68 compounds which paved the way towards the endotherapy applications.

6. PHOSPHO(I)NATE AND THIOL-BASED INHIBITORS

In the early 2000s studies on GCPII inhibitors aimed to find a treatment for neurological disorders associated with glutamate excitotoxicity [37-39].

Based on the substantial evidence that GCPII is a metallopeptidase, pharmaceutical researchers originally focused on the synthesis of small molecules containing functional groups with known capability to inhibit metallopeptidases, such as hydroxyphosphinyl derivatives, thiol derivatives, and hydroxamic acids [37].

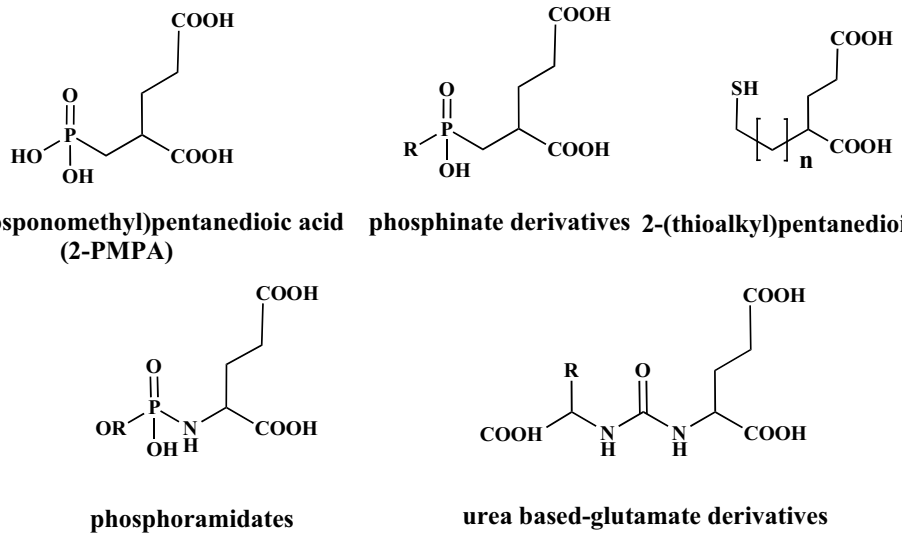

Fig. (2). Chemical sturctures of the main classes of PSMA small-molecule ligands.

Among these compounds, 2-(phosphonomethyl)pentanedioic acid (2-PMPA) showed the highest pharmacologic activity, more than 1000 folds potent than previously described inhibitors [37]. Its exceptional efficacy is attributed to the strong chelation of the phosphonate group to the zinc ion active-site, as well as the interaction of the glutarate (pentanedioic acid) moiety of the inhibitor (P1' region) with the glutamate recognition site of GCPII (S1' pocket) [38].

Despite the optimal premises as a candidate for the inhibitor of the enzyme, penetration into the brain through the blood-brain barrier was found to be limited, likely hampered by the polar nature of 2-PMPA. In order to obtain more lipophilic compounds and hopefully, a more favorable pharmacokinetics profile, extensive SAR studies using 2-PMPA as a template were carried out, generating a new class of potent phosphinate-based inhibitors of GCPII [39]. The relatively poor pharmacokinetics of these compounds and their limited potential as therapeutics, induced researchers to shift their efforts on different classes of molecules with an enhanced oral bioavailability [38]. Considering that thiols are among the most extensively and successfully studied metalloprotease inhibitors, as showed by inhibitors of angiotensin converting enzyme (*e.g.* captopril), studies were driven in order to replace the phosphonomethyl group of 2-PMPA with thioalkyl groups [38].

These investigations led to the development of 2-(thioalkyl)pentanedioic acids and other analogues. The GCPII inhibitory potency of these compounds was found to be dependent on the number of methylene units between the thiol group and pentanedioic acid [38].

From this initial lesson after the above mentioned studies on phosphonate-, phosphinate- compounds and thiols at least two features are essential for the development of potent inhibitors of PSMA: a strong zinc binding group for the interaction with the active-site of the enzyme and a glutarate moiety in the P1' position for the binding with the S1' pocket [15]. Certainly much work needs to be done for approaching at an efficient drug discovery, but all these information have been useful for the design of the other class of inhibitors.

7. GLUTAMATE-PHOSPHORAMIDATE INHIBITORS

The identification of the hydrophobic accessory pocket using a series of phenylalkylphosphonamidate derivatives of glutamic acid as hydrophobic probes, inspired the exploration of substituted phosphoramidates as transition-state analog inhibitors of PSMA [40].

As previously mentioned above, a glutamate residue at P1' appears essential to ensure the interaction between the γ-carboxylate and Asn-257 and Lys-699, as well as the α-carboxylate group with Arg-210 [40].

The incorporation of the phosphoramidate function, as a zinc-coordinating group for the PSMA active site, was observed to promote the binding affinity if compared to phosphonates and phosphinates. This is likely due to the presence of two additional hydrogen bonds between the phosphoramidate nitrogen and carboxylate of Glu-424 and the Gly-518 carbonyl oxygen, respectively [35]. P1′ glutamate residue and the phosphoramidate showed to be critical for ensuring the binding, the P1 group (which specifically interacts with the S1 pocket) was found to be important to define the PSMA inhibition level [40].

Liu *et al*. [41] demonstrated that inhibitors including a hydrophobic residue and a carboxylate in the P1 moiety exhibit pseudo-irreversible inhibition of PSMA activity, while phosphoramidate peptidomimetics lacking either a P1 carboxylate or hydrophobic group exhibit a moderately reversible inhibition.

In the details, as revealed by docking studies, the presence of a P1 hydrophobic group induces π-stacking or hydrophobic interactions with nearby aromatic residues (Tyr-234, Tyr-549, Tyr-552 and Tyr-700) while the P1 carboxylate provides an additional interaction with Arg-536 [40, 41].

An irreversible binding profile is desirable because it might induce a higher rate of internalization than weaker interaction and consequently, rapid *in vivo* tumor uptake after the administration and greater contrast with the background tissues [42]. Conversely, reversible binding may ex-

plain the tumor washout over several hours observed with urea-based inhibitors [43].

As an exception to the above criteria based on in silica studies, CTT54 is an interesting inhibitor lacking a hydrophobic residue in the P1 moiety, but including a glutamate residue linked by the γ-carboxylate to the serine via the peptide bond. Despite its intrinsic flexibility, the γ-glutamate linker position is defined by a network of interactions with residues lining the GCPII binding cavity (Fig. **3**). In addition, the free N-terminal group allows CTT54 conjugation with groups with different physicochemical characteristics leading to the increase of inhibitor affinity towards GCPII [35].

Several CTT54 derivatives have been radiolabeled with ^{18}F and ^{99m}Tc in order to obtain potential PET [42-44] and SPECT [45] imaging agents for PCa respectively.

Ganguly *et al.* synthesized a promising derivative [^{18}F]CTT1057 including a p-Fluorobenzoyl-aminohexanoate and a 2-(3-hydroxypropyl)glycine into the PSMA-targeting scaffold. X-ray crystallography revealed π-stacking and π−cationic interaction of the fluorobenzamido (FB) ring with the Arg 511/Try 541 and Arg 463 residues, at the arene-binding site (ABS) (Fig. **3**). This additional and peculiar interaction was thought to be responsible for enhanced PSMA affinity and favorable *in vivo* characteristics of this radiotracer compared to other previous reported [42].

A series of FB ring-containing compounds derivative of CTT1057 were designed in order to further understand the SAR of phosphoramidates respect to the interactions within the ABS and to evaluate their corresponding *in vivo* pharmacokinetics and biodistribution [43].

Detailed information regarding the modality of interaction was collected, however, [^{18}F]CTT1057 remained the most prominent tracer of this class, due to its optimal binding, tumor uptake and retention, and remarkable tumor-to-blood ratios.

A phase I study (ClinicalTrials.gov, NCT02916537) is already completed in patients with prostate cancer prior to radical prostatectomy and in patients with metastatic castration resistant prostate cancer (mCRPC). [^{18}F]CTT1057 detected mCRPC lesions in the soft tissue and bone at greater sensitivity than conventional imaging and showed similar biodistribution to ureido-based PSMA-targeted agents, with preliminary evidence of lower uptake in the salivary gland and kidney [46].

8. GLUTAMATE-UREIDO-BASED INHIBITORS

Glutamate-ureido (Glu-ureido) based inhibitors are by far the most explored class of PSMA agents. Several radioligands have already entered advanced clinical settings both in diagnosis and in therapy, although to date a full approval by regulatory authorities has not yet reached neither in Europe nor in USA.

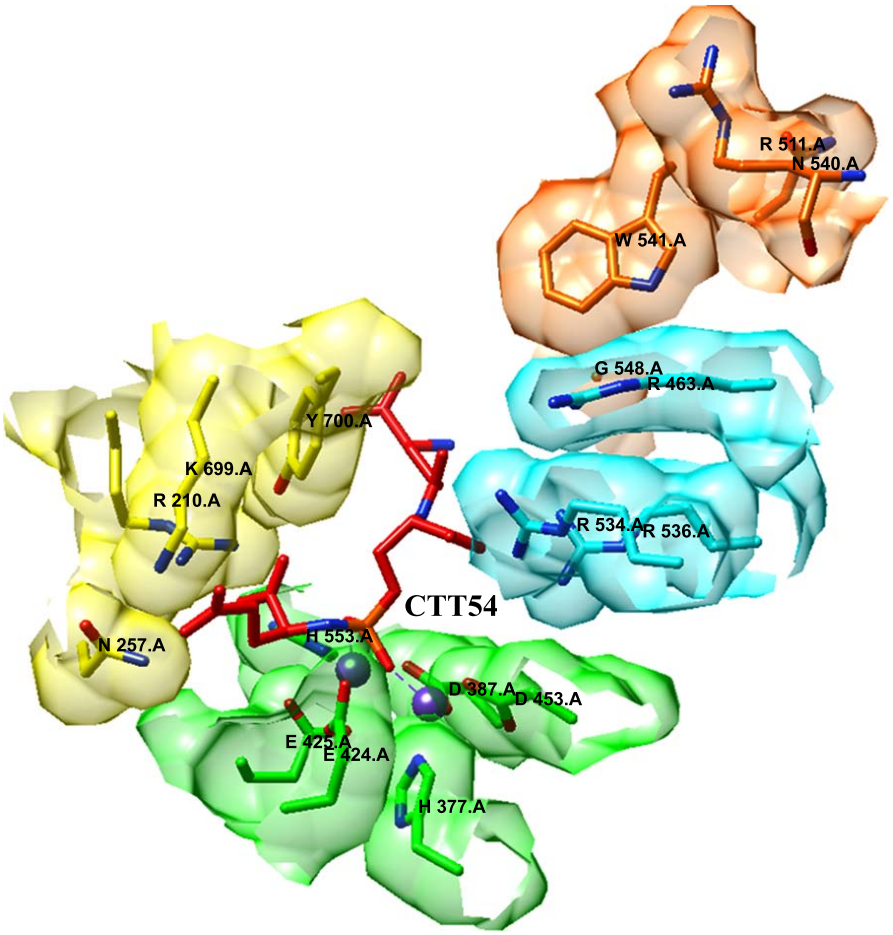

Fig. (3) contd….

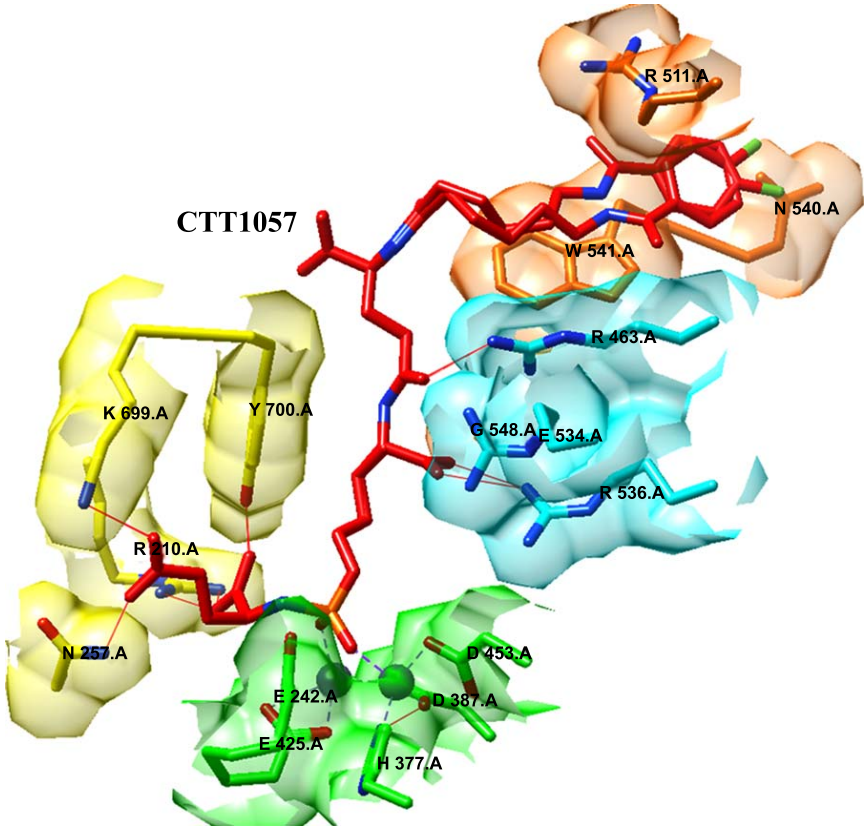

Fig. (3). CTT54 (PDB code 4P4B) and CTT1057 (PDB code 4JYW) interactions with the main residues lining the internal cavity of human GCPII. Inhibitors are coloured in red; the S1' pocket residues in yellow; the active site in green; the arginine patch in cyan and the entrance lid in orange. All the residues and the ligands are in stick representation. The figure shows the CTT1057 interactions with the ABS residues inside the entrance lid, responsible of the its enhanced PSMA affinity (realized by UCSF Chimera).

Inspired by NAAG structure, Kozikowski *et al*. designed and synthesized a dually acting ligand, 4,4′-phosphinicobis-(butane-1,3-dicarboxylic acid), which acts both as a selective agonist for the metabotropic glutamate receptor (mGluR3) and as a potent inhibitor of GCPII [47]. From this lead compound, the phosphinic core $H_2P(O)(OH)CH_2$, was replaced by an ureido group [47] in order to mime a planar peptide bond of a GCPII substrate, such as NAAG, but with improved resistance to enzymatic hydrolysis [34].

Based on this design framework N-[N-[(S)-1,3-dicarboxypropyl]carbamoyl]-(S)-[^{11}C]methyl-L-cysteine ([^{11}C]DCMC) has been the first reported radiolabeled inhibitor [6].

The constraints due to the short physical half-life of carbon-11, suggested to shifting towards radioligands containing a different radioisotope. Therefore, [^{11}C]DCMC has been rapidly followed by N-[N-[(S)-1,3-dicarboxypropyl]carbamoyl]-(S)-3-[^{125}I]iodo-L-tyrosine ([^{125}I]DCIT), a SPECT tracer more suitable for clinical application. Iodide-125 ($t_{1/2}$ = 59.49 days) was chosen for its low cost and availability [25], and more interestingly, because its labeling chemistry can be easily switched to Iodide-123 or Iodide-124 for human SPECT or PET, respectively [7], or to iodide-131 for a theragnostic approach.

Both [^{11}C]DCMC and [^{125}I]DCIT exhibited specific uptake in human prostate cancer xenografts thus generating attention for this class of new compounds, and for its great potential for nuclear medicine applications [48]. These first results promoted the development of other Glu-ureido-based inhibitors, which came in quick succession without a break during the following years.

8.1. Fluorine-18 Glu-Ureido Based Derivatives

[^{18}F]fluorobenzyl-derivative of DCMC, N-[N-[(S)-1,3-dicarboxypropyl]carbamoyl]-(S)-4-[^{18}F]fluorobenzyl-L-cysteine or [^{18}F]DCFBC, was synthesized in order to exploit the characteristics of fluorine-18 for clinical translation. [^{18}F]DCFBC enabled visualization of PSMA positive PC3 PIP tumor xenografts with negligible non-target organ uptake, except for kidney and limited radioactive accumulation within the bladder [6].

Unfortunately, a relevant [^{18}F]DCFBC drawback is the strong binding with serum proteins, determining a long blood clearance time, which reduces tumor-to-background ratio [49].

A second generation agent, the 2-(3-{1-carboxy-5-[(6-[^{18}F]fluoro-pyridine-3-carbonyl)-amino]-pentyl}-ureido)-pentanedioic acid, known as [^{18}F]DCFPyL, was developed to overcome this limitation [50]. It contains a 6-[^{18}F]fluoronicotinamido group on a lysine-glutamate urea and demonstrated not only a lower permanency in the blood pool, but

also a substantially greater binding affinity for PSMA and a higher tumor uptake, if compared to [^{18}F]DCFB [50, 51].

DCFBC and DCFPyL, as well as DCMC and DCIT structures belong to the same class of non-hydrolysable analogues of NAAG, which differ for the N-acetylaspartate moiety replaced by four different side chains.

The common features and the peculiarities of interaction for each compound within the enzymatic pocket have been highlighted through SAR studies using recombinant human GCPII (rhGCPII) (Fig. **4**) [34].

First, the interactions of α- and γ-carboxylate groups of the urea inhibitors with the side chains of amino acids in the S1' pocket are virtually identical to those observed for complexes of rhGCPII with free glutamate and phospho(i)nate analogues of glutamate/NAAG. This observation confirms that the S1′ pocket is "optimized" for glutamate binding, and glutamate-like residues are the best choice if positioned at the C-terminus of GCPII inhibitors.

Secondary the active-site re-arrangement of the rhGCPII-ureido complexes reflects the situation of the native rhGCPII (E424A)/NAAG complex with the distance between the two active-site zinc ions ~3.3 Å and an activated water molecule positioned symmetrically in between them (2.0 Å). This finding validates the prediction of the urea biostere as a surrogate of the peptide bond.

In conclusion, the C-terminal glutamate and the ureido group of all four inhibitors structurally overlap and the different behaviors are related to some substantial differences within the S1 "hydrophobic pocket" of the enzyme.

The only common feature of the S1 sites in the four complexes concerns the interactions of the P1 carboxylate with the side chains of Asn-519, Arg-534 and Arg-536 and two water molecules. Except for the P1 methylcysteine side chain of DCMC for which no significant interactions into the "hydrophobic pocket" of the S1 pocket were observed, DCIT, DCFBC, and DCIBzL showed a phenyl ring as a terminal part of their P1 side chain. They differ in the length of the linker connecting the ring to the ureido group: the linker in DCIT consists of only one methylene group, while those of DCFBC and DCIBzL include three and six methylene groups, respectively. Consequently, the phenyl groups of DCFBC, and especially of DCIBzL, have more positional freedom and could extend further into the hydrophobic pocket of S1 site (Fig. **4**).

[^{18}F]DCFBC application has been investigated in a limited number of Clinical trials (ClinicalTrials.gov, NCT01417182, NCT01815515, NCT01496157, NCT02190279) [49, 52, 53], while [^{18}F]DCFPyL is by far the most studied being used in more than 30 ongoing studies.

More recently, a novel fluorinated compound with a different rationale in the design, and peculiar biological properties, has been introduced in the clinical setting. [^{18}F]PSMA-1007 development is based on the chemical structure of PSMA-617 (which will be discussed later) (Fig. **5**). It shares the Glu-urea-Lys motif targeting the PSMA enzymatic

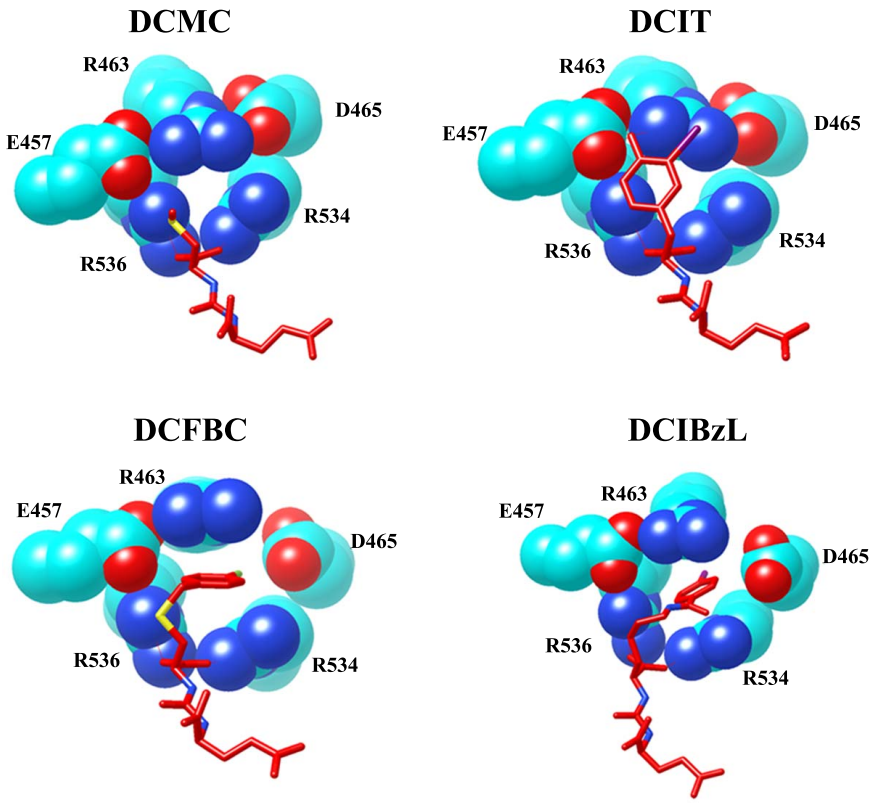

Fig. (4). Hydrophobic accessory pocket of GCPII in complex with DCMC, DCIT, DCFBC and DCIBzL (realized by UCSF Chimera. PDB code 3D7G, 3D7F, 3D7D, 3D7H). Pocket residues (R463, R534, R536, D465, E457) are shown as spheres (cyan) and inhibitors are in stick representation (red). The figure shows the Arg-463 side chain switch from "down" to "up" position in DCFBC and DCIBzL structures, due to the presence of longer P1 spacer.

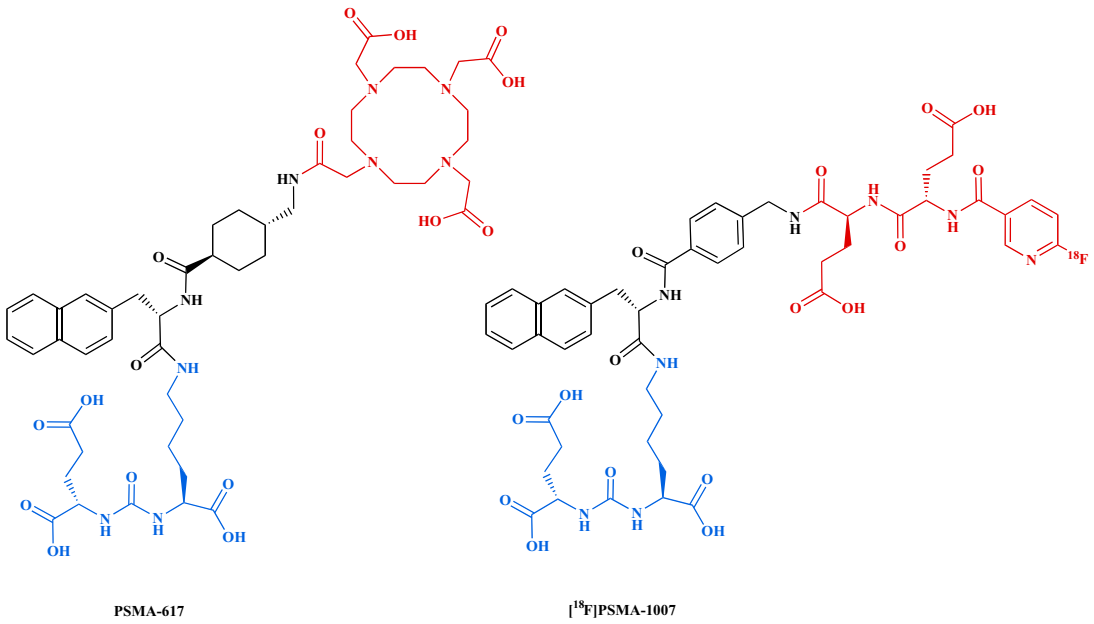

Fig. (5). Chemical structures of PSMA-617 ligand and [^{18}F]PSMA-1007.

pocket S1' and the naphthalene-based linker region considered to co-target the hydrophobic accessory pocket S1. The main difference relies on the radiolabel-bearing moiety, where two glutamic acids were added to mimic the carboxylic acid groups of the DOTA chelator [54].

The ligand showed promising binding and internalization properties *in vitro* as well as high and specific uptake *in vivo* [55]. Furthermore, PSMA-1007 presents a unique biodistribution compared to the other known PSMA-ligands, because excretion follows almost exclusively the hepatobiliary pathway. This might represents facilitation in the differentiation of lymph node metastases of recurrent PCa from urinary activity or for the differentiation of local relapse from the urinary bladder [56, 57]. [^{18}F]PSMA-1007 might also be ideally used as a theragnostic match pair with [^{177}Lu]PSMA-617, thanks to chemical structure and *in vivo* distribution similarities. Further studies will define the importance of this radioligand, which appears very promising for an application in the clinical setting [55, 56, 58, 59].

8.2. Glu-Ureido Based Derivatives for Nuclear Medicine Conventional Imaging

During the last decade, researchers turned their attention to modifications at the linker/functional spacer/effector portion of Glu-ureido based ligands [36]. Unlike the constricted S1' glutamate recognition pocket, the entrance funnel is able to accommodate several chemical groups with different capabilities of modulating the binding affinities. The aminohexanoyl moiety was typically used as the proximal segment of the linker to form 2-[3-(5-amino-1-carboxy-pentyl)-ureido]- pentanedioic acid (Lys-C(O)-Glu- or KuE) derivatives [7]. Its flexibility enables "optimized positioning" of coupled functional spacers or effector moieties within the amphipathic entrance funnel. Additionally, the engagement of these moieties with structurally defined pockets in the entrance funnel is facilitated (*i.e.* for the S1 accessory hydrophobic pocket or the arene-binding site), thus contributing to the increased affinity of such PSMA ligands [36].

The conjugation between the KuE linker and suitable radiolabeled prosthetic groups (4-[^{125}I]iodo-benzoyl, 4-[^{18}F]fluoro-benzoyl and the 5-[^{125}I]iodo-3-carbonyl-pyridine) by the reaction on the ε-amino group of lysine, led to the development of several radiohalogeneted agent both for SPECT and PET imaging, as described by Chen *et al*. [7].

MIP-1072 ((S)-2-(3-((S)-1-carboxy-5-(4-iodobenzylamino) pentyl)ureido) pentanedioic acid) and MIP-1095 ((S)-2-(3-((S)-1-carboxy-5-(3-(4-iodophenyl)ureido)pentyl)ureido) pentanedioic acid) (Fig. **6**) [48] were identified as potential ligands for targeting PSMA, indicating a new direction towards the development of clinically viable labeled PSMA agents.

The labeled derivatives [^{123}I]MIP-1072 and [^{123}I]MIP-1095 showed a rapid detection of lesions in soft tissues, bone, and prostate gland in patients with histopathology or radiologic evidence of metastatic PCa [60]. The excellent affinities (very low nanomolar) and selective binding exhibited by this class of new inhibitors led to investigate the feasibility in developing ^{99m}Tc-labeled urea-based inhibitors as PCa imaging agents [61].

^{99m}Tc remains the radionuclide of choice for scintigraphy because of its favorable physical properties ($t_{1/2}$ = 6h), low cost, and widespread availability. Several ^{99m}Tc-PSMA agents including the KuE motif were developed and tested. Structural variations involved (a) the length of the linker between the chelator and the amide carbonyl attached to the lysine moiety, (b) the nature of chelator, (c) the presence of a second amide group between the chelator and the first amide-to the lysine moiety, and (d) the presence of a carboxyl group either adjacent to the chelator or to the second (linker) amide group [62].

Moreover from *in vitro* binding studies emerged the need to insert a functionalized methylene linker (>20 Å), long enough to preserve the urea moiety binding to the active site and keeping the bulky metal chelated part on the exterior of the enzyme [61, 62].

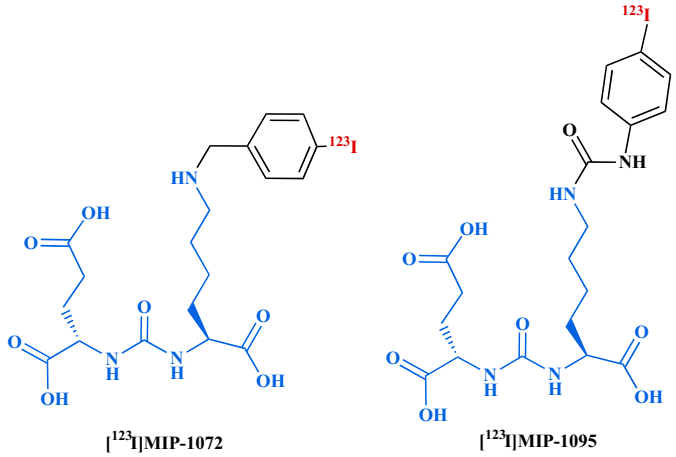

Fig. (6). Chemical structures of [^{123}I]MIP-1072 and [^{123}I]MIP-1095.

At least three different class of ^{99m}Tc complexes were developed to investigate the chelator impact on the biodistribution and PCa tumor uptake, including ^{99m}Tc(I)tricarbonyl core ([^{99m}Tc(CO)$_3$]$^+$) using hydrophilic ligands, ^{99m}Tc(V)-oxo ([^{99m}TcO]$^{3+}$) core via traditional N_xS_y-based chelating agents and ^{99m}Tc(III)-organohydrazine(^{99m}Tc-hynic) - labeling [63].

The most successful class of ^{99m}Tc-PSMA agents was developed by Hillier *et al*. whom synthesized and evaluated a series of novel Single-Amino-Acid Chelators (SAACs), including carboxylic acid-substituted imidazoles, with improved pharmacokinetic properties [64].

The Glu-urea-Glu or Glu-urea-Lys pharmacophores were conjugated with two different SAACs, CIM (2,2'-(2,2'-(azanediylbis(methylene))bis(1H-imidazole-2,1-diyl)) diacetic acid) and TIM (2,2',2'',2''' -((2,2'-(2,2'-(azanediylbis (methylene))bis(1Himidazole-2,1-diyl))bis(acetyl))bis(azanetriyl)) tetraacetic acid). The resulting ligands were then radiolabeled with technetium-99m tricarbonyl core: the structures of [^{99m}Tc]MIP-1405 and [^{99m}Tc]MIP-1427 incorporate the CIM chelate, while the structures of MIP-1404 and MIP-1428 contain the TIM chelate (Fig. **7**).

All compounds exhibited high affinity and specificity for PSMA and internalization upon binding to PSMA in LNCaP cells. However the more hydrophilic TIM chelate, containing an additional carboxylic acid group with respect the CIM structure, was synthesized in order to enhance renal clearance and further decrease of non-target signal [64].

Among the examined compounds, [^{99m}Tc]MIP-1404 displayed the best performances as diagnostic agents, becoming a promising candidate for approaching to a clinical application [64]. [^{99m}Tc]MIP-1404, also known as Trofolastat™, has been investigated in several clinical trials resulting as the first PSMA imaging agent to finalize phase 3 clinical trials (ClinicalTrials.gov, NCT02615067). It is therefore expected that [^{99m}Tc]MIP-1404 (Trofolastat), available as a "technetium instant kit", will be likely launched on the market very soon.

8.3. Gallium-68 Glu-Ureido Based Derivatives

The successfully experience with the Lys-Urea-Glu moiety have been also extended towards the development of ^{68}Ga-based PET agents for PCa imaging [65]. In recent years, gallium-68 has gained importance in molecular imaging due to the favorable emitting properties, the established Ga^{3+} coordination chemistry and the widespread presence of^{68}Ge/^{68}Ga generator in radiopharmacies [66]. A number of chelators are currently used for gallium-68 stabilization and the concomitant conjugation with carrier molecules for clinical and preclinical diagnostics, as well as in therapeutics [67].

Among these, DOTA is still considered the gold standard for gallium-68 because of its availability, flexibility and a well-known coordination chemistry [66]. Banerjee *et al*. synthesized two [^{68}Ga]DOTA-conjugated PSMA inhibitors, differentiated by the linker between the Lys-Urea-Glu moiety and the chelator with maintained specificity for the PSMA enzymatic pocket. Similarly to the case of technetium PSMA agents, the presence of the linker is recognized as critical to direct the gallium complex through the 20 Å tunnel away from the active site [65]. This is not just because of the structural requirements of the S1 hydrophobic pocket, but also for the considerable dimension of the whole metal complex, which is clearly bulky if compared with a radiohalogen.

A compromise in between the structural manipulation of the linker and the stabilization of the gallium-metal core has been achieved with the design of new ligands, implemented with the more efficient chelator, but less explored, HBED-CC (N,N'-Bis[2-hydroxy-5-(carboxyethyl)- benzyl]ethylenediamine-N,N'- diacetic acid) [67].

Due to its capability to enhance the overall lipophilicity of the resulting radioligand, which corresponds to increased binding properties, HBED-CC became quickly the chelator of choice for gallium-68 based PSMA tracers [26].

The most prominent example of PSMA-specific agent is the amphiphilic tracer [^{68}Ga]PSMA-11 (also known as [^{68}Ga]PSMA-11 or [^{68}Ga]Glu-Urea-Lys(Ahx)-HBED-CC), consisting of the urea-based pharmacophore and the [^{68}Ga]HBED-CC complex (Fig. **8**), able to directly interact with the hydrophobic binding pocket S1.

[^{68}Ga]PSMA-11 exhibited a similar binding affinity if compared to the two [^{68}Ga]DOTA-PSMA inhibitors previously reported, but a concomitant reduced non-specific binding and considerable higher internalization in LNCaP cells

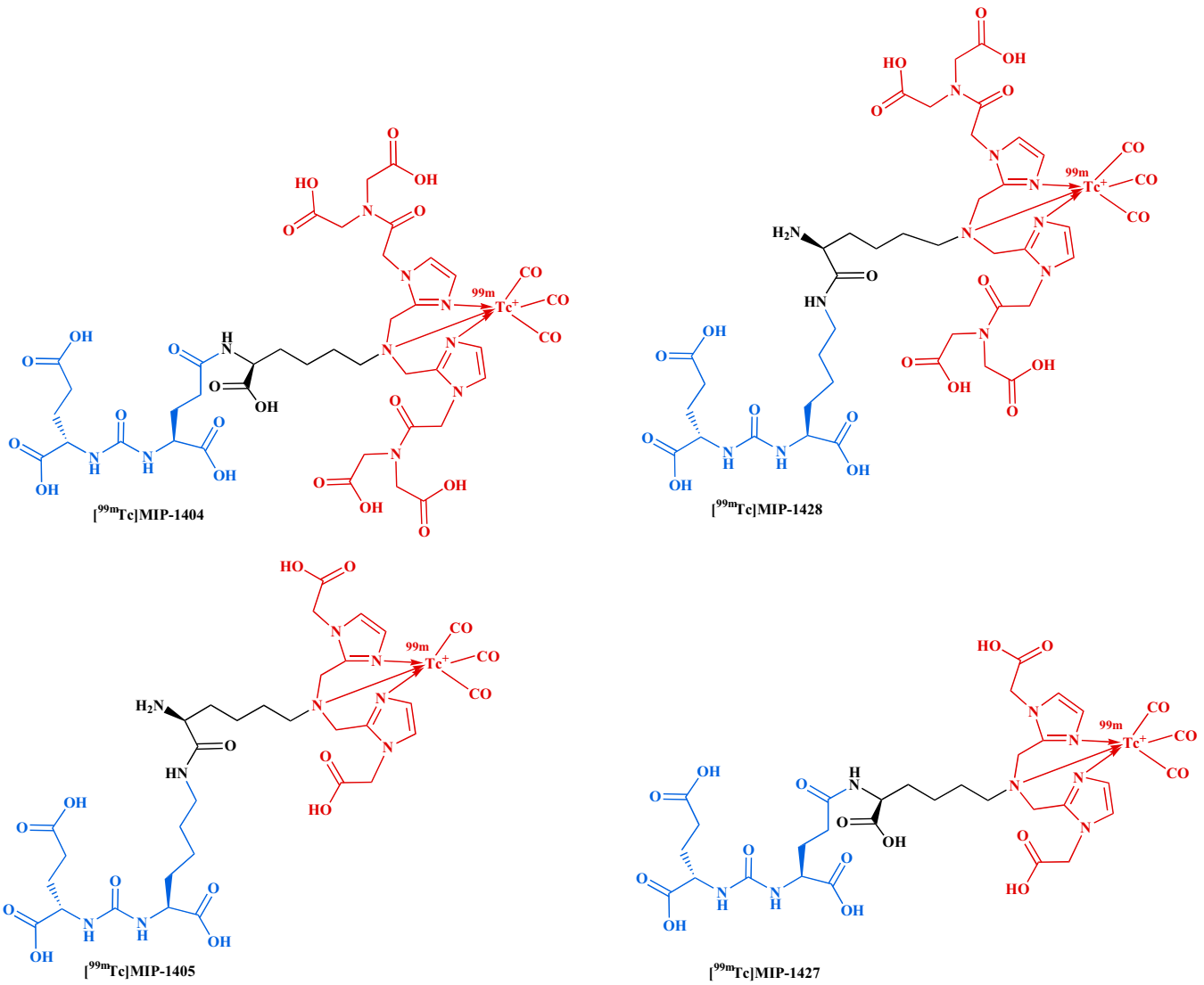

Fig. (7). Chemical structures of [^{99m}Tc]MIP-1404, [^{99m}Tc]MIP-1428, [^{99m}Tc]MIP-1405 and [^{99m}Tc]MIP-1427.

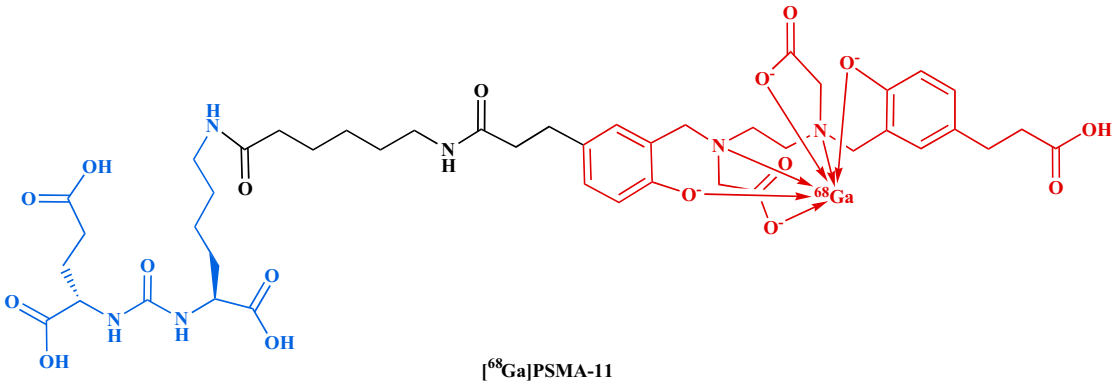

Fig. (8). Chemical structure of [^{68}Ga]PSMA-11.

[67]. Hydrophobic interactions of aromatic residues of HBED-CC complex seem to be responsible for the improved binding properties of [^{68}Ga]PSMA-11, while the rate of internalization depends on the conformational changes of PSMA induced by inhibitor binding at the S1' pocket.

All these *in vitro* evidences were also confirmed by *in vivo* studies, where the radiolabeled compound exhibited fast blood and organ clearances, low liver accumulation, and high specific uptake in PSMA expressing organs and tumor [67].

In addition to the optimal kinetic performances, there are some technical aspects which corroborate the use of [^{68}Ga]PSMA-11 in the clinical practice. PSMA-11 can be easily radiolabeled with ^{68}Ga(III) at room temperature in few minutes in high yield and purity [6], using remote controlled synthesizers or "instant kits", which have been already developed although not yet commercially available.

As a major consequence [^{68}Ga]PSMA-11 has been largely investigated as a diagnostic agent in all stages of PCa and it is notably that a monograph for [^{68}Ga]PSMA-11 is currently under evaluation by the European Pharmacopoeia (EDQM, European Directorate for the Quality of Medicine), pending for final approval hopefully within the next year.

8.4. Glu-Ureido Based Derivatives for Nuclear Medicine Endoradiotherapy

Despite [^{68}Ga]PSMA-11 proved to be a successful tracer for PET imaging, the employed ligand PSMA-11 is not suitable for radiolabeling with therapeutic radiometals such as ^{177}Lu or ^{90}Y [68]. In order to overcome this constraint, Benešová *et al*. reported the synthesis and preclinical evaluation of PSMA-617, a theragnostic ligand, in which the chelator DOTA was conjugated to the pharmacophore Glu-urea-Lys by a naphthalic spacer [68]. The study showed that the insertion of the naphthyl function in the linker has a significant impact on the tumor-targeting, as well as on the pharmacokinetics, thus resulting in an improved imaging contrast. Regarding the therapeutic applications, at the beginning mainly with lutetium-177, the high binding affinity and internalization, together with a prolonged tumor uptake and rapid kidney clearance suggested that PSMA-617 represented a marked advance if compared with previously published DOTA-based PSMA inhibitors. In summary, PSMA-617 seems to be more suitable for endoradiotherapy (ERT) because of its higher tumor uptake at later time points, lower spleen accumulation, and highly efficient clearance from the kidneys [68].

[^{177}Lu]PSMA-617 has been evaluated in phase I studies for its dosimetry, safety, and efficacy as a diagnostic agent, as well as response and tolerability in its therapeutic application [69-72]. Its use for radionuclide treatment in metastatic castration-resistant PCa has been considered promising, particularly in patients with a progression of the disease after standard treatments [71, 72]. PSMA-617 is being commonly investigated due to its versatility for both diagnostic (with gallium-68 and fluorine-18, see the development of PSMA-1007 described before) and therapeutics.

However, some studies have demonstrated a general lower tumor uptake, mainly if compared with HBED-CC chelated agents [67].

In order to further improve ligand pharmacokinetics and obtain labeled derivatives with higher affinity, a Lys-Urea-Glu (KuE) scaffold coupled to the spacer Phe-Phe-Lysine-suberoyl (L-amino acid spacer, FFK-Sub), was functionalized with the chelator 1,4,7,10-tetraazacyclododececane,1-(glutaric acid-4,7,10-triacetic acid (DOTAGA), termed DOTAGA-FFK(Sub-KuE) [73].

[^{68}Ga]DOTAGA-FFK showed a fast metabolism *in vivo*, resulting in discontinuous clearance kinetics and low tumor accumulation, which is consistent with *in vivo* results obtained with other PSMA ligands including in the structure L-amino acid spacers [73]. Since this problem is believed to rely on a rapid proteolytic cleavage, the L-amino acid spacer was replaced by its D-amino acids counterpart resulting in a ligand with high metabolic stability *in vivo*. In addition, DOTAGA-conjugated ligands showed a significantly increased affinity towards PSMA on LNCaP cells compared to the DOTA analogues [73].

The further substitution of the D-phenylalanine residues in the peptidic linker by 3-iodo-D-tyrosine enhanced the interaction with the binding site, leading to the optimized ligand DOTAGA-(I-y)fk(Sub-KuE) (Fig. **9**) [74]. It is also known as PSMA I&T (PSMA I&T for Imaging &Therapy), since it can be labeled with both the diagnostic radionuclide ^{68}Ga and the therapeutic radionuclide ^{177}Lu.

This agent, like PSMA-617, allows a theragnostic approach to prostate cancer diagnosis and treatment. The clinical efficacy of [^{68}Ga]PSMA-I&T appears equivalent to [^{68}Ga]PSMA-HBED though imaging characteristics appear slightly better for the latter imaging agent [75]. Both tissue distribution pattern and time of accumulation are comparable to PSMA-11. Furthermore, similar to [^{68}Ga]PSMA-11, [^{68}Ga]PSMA-I&T demonstrates predominantly renal excretion [74].

Some clinical trials have been assessed the use of [^{68}Ga]PSMA-I&T PET/CT for the detection of primary PCa before prostatectomy [76] and BCR [77-78].

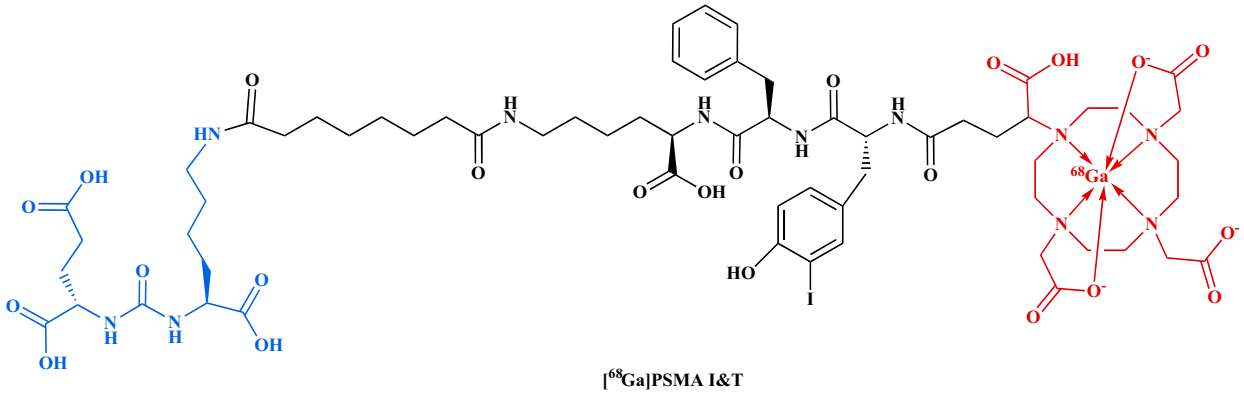

Fig. (9). Chemical structure of [^{68}Ga]PSMA-I&T.

CONCLUSION

PSMA represents the most attractive target for the detection and treatment of patients affected by PCa using nuclear medicine modalities. Due to a dramatic scientific advancement in the knowledge of PSMA structural conformation and interaction mechanism with synthetic inhibitors, a variety of radiometal and radiohalogen-based PSMA ligands for PET as well as SPECT imaging have been developed and tested till date.

[^{99m}Tc]MIP-1404 (^{99m}Tc-Trofolastat) seems to be the tracer of choice for SPECT imaging of prostate cancer, while [^{68}Ga]PSMA-11 was identified as a leading diagnostic candidate for non-invasive PET imaging of prostate cancer.

[^{18}F]DCFPyL and [^{18}F]PSMA-1007 are also considered promising PET PSMA tracer, with the potential of commercial distribution and a more capillary distribution to PET centers without cyclotron or gallium-68 technology. Favored by a delayed renal excretion, their employment might be useful for patients in which local recurrence cannot be differentiated from activity by urinary tracer excretion.

More recently, researches are also focusing on the development of PSMA inhibitors for a theragnostic application, suitable for both radiolabeling with diagnostic (Gallium-68, Fluorine-18) and therapeutic radionuclides (Lutetium-177, Actinium-225).

To date, both [^{68}Ga]PSMA-11 and PSMA-617 (^{177}Lu or ^{225}Ac labeled) principally cover the diagnostic and therapeutic aspects of clinical prostate cancer care.

CONSENT FOR PUBLICATION

Not applicable.

FUNDING

None.

CONFLICT OF INTEREST

The authors declare no conflict of interest, financial or otherwise.

ACKNOWLEDGEMENTS

Declared none.

REFERENCES

[1] International Agency for Research on Cancer. World Health Organization. Global cancer observatory: Cancer Today.. https://gco.iarc.fr/today/data/factsheets/populations/900-world-fact-sheets.pdf [Accessed April 08, 2019].

[2] Babich, J.W.; Joyal, J.L.; Coleman, R.E. Targeting prostate cancer with small molecule inhibitors of prostate -specific membrane antigen In: *Targeted Molecular Imaging;*; Welch , M. J.; Eckelman, W. C., Eds.; Taylor & Francis Group, LLC: Lenexa, **2012**; pp. 161-174.

[3] Spratt, D.E.; McHugh, D.J.; Morris, M.J.; Morgans, A.K. Management of Biochemically Recurrent Prostate Cancer: Ensuring the Right Treatment of the Right Patient at the Right Time. *Am. Soc. Clin. Oncol. Educ. Book,* **2018**, *38*, 355-362. [http://dx.doi.org/10.1200/EDBK_200319] [PMID: 30231323]

[4] Ilic, D.; Djulbegovic, M.; Jung, J.H.; Hwang, E.C.; Zhou, Q.; Cleves, A.; Agoritsas, T.; Dahm, P. Prostate cancer screening with prostate-specific antigen (PSA) test: a systematic review and meta-analysis. *BMJ,* **2018**, *362*, k3519. [http://dx.doi.org/10.1136/bmj.k3519] [PMID: 30185521]

[5] Eastham, J. Prostate cancer screening. *Investig. Clin. Urol.,* **2017**, *58*(4), 217-219. [http://dx.doi.org/10.4111/icu.2017.58.4.217] [PMID: 28681029]

[6] Kiess, A.P.; Banerjee, S.R.; Mease, R.C.; Rowe, S.P.; Rao, A.; Foss, C.A.; Chen, Y.; Yang, X.; Cho, S.Y.; Nimmagadda, S.; Pomper, M.G. Prostate-specific membrane antigen as a target for cancer imaging and therapy. *Q. J. Nucl. Med. Mol. Imaging,* **2015**, *59*(3), 241-268. [PMID: 26213140]

[7] Chen, Y.; Foss, C.A.; Byun, Y.; Nimmagadda, S.; Pullambhatla, M.; Fox, J.J.; Castanares, M.; Lupold, S.E.; Babich, J.W.; Mease, R.C.; Pomper, M.G. Radiohalogenated prostate-specific membrane antigen (PSMA)-based ureas as imaging agents for prostate cancer. *J. Med. Chem.,* **2008**, *51*(24), 7933-7943. [http://dx.doi.org/10.1021/jm801055h] [PMID: 19053825]

[8] Mease, R.C.; Foss, C.A.; Pomper, M.G. PET imaging in prostate cancer: focus on prostate-specific membrane antigen. *Curr. Top. Med. Chem.,* **2013**, *13*(8), 951-962. [http://dx.doi.org/10.2174/1568026611313080008] [PMID: 23590171]

[9] Cuccurullo, V.; Di Stasio, G.D.; Mansi, L. Nuclear Medicine in Prostate Cancer: A New Era for Radiotracers. *World J. Nucl. Med.,* **2018**, *17*(2), 70-78. [PMID: 29719480]

[10] Foss, C.A.; Mease, R.C.; Cho, S.Y.; Kim, H.J.; Pomper, M.G. GCPII imaging and cancer. *Curr. Med. Chem.,* **2012**, *19*(9), 1346-1359. [http://dx.doi.org/10.2174/092986712799462612] [PMID: 22304713]

[11] Schuster, D.M.; Nanni, C.; Fanti, S. Evaluation of Prostate Cancer with Radiolabeled Amino Acid Analogs. *J. Nucl. Med.,* **2016**, *57*(Suppl. 3), 61S-66S. [http://dx.doi.org/10.2967/jnumed.115.170209] [PMID: 27694174]

[12] Afshar-Oromieh, A.; Babich, J.W.; Kratochwil, C.; Giesel, F.L.; Eisenhut, M.; Kopka, K.; Haberkorn, U. The Rise of PSMA Ligands for Diagnosis and Therapy of Prostate Cancer. *J. Nucl. Med.,* **2016**, *57*(Suppl. 3), 79S-89S. [http://dx.doi.org/10.2967/jnumed.115.170720] [PMID: 27694178]

[13] Bařinka, C.; Rojas, C.; Slusher, B.; Pomper, M. Glutamate carboxypeptidase II in diagnosis and treatment of neurologic disorders and prostate cancer. *Curr. Med. Chem.,* **2012**, *19*(6), 856-870. [http://dx.doi.org/10.2174/092986712799034888] [PMID: 22214450]

[14] Tykvart, J.; Schimer, J.; Bařinková, J.; Pachl, P.; Poštová-Slavětínská, L.; Majer, P.; Konvalinka, J.; Šácha, P. Rational design of urea-based glutamate carboxypeptidase II (GCPII) inhibitors as versatile tools for specific drug targeting and delivery. *Bioorg. Med. Chem.,* **2014**, *22*(15), 4099-4108. [http://dx.doi.org/10.1016/j.bmc.2014.05.061] [PMID: 24954515]

[15] Mesters, J.R.; Barinka, C.; Li, W.; Tsukamoto, T.; Majer, P.; Slusher, B.S.; Konvalinka, J.; Hilgenfeld, R. Structure of glutamate carboxypeptidase II, a drug target in neuronal damage and prostate cancer. *EMBO J.,* **2006**, *25*(6), 1375-1384. [http://dx.doi.org/10.1038/sj.emboj.7600969] [PMID: 16467855]

[16] Ghosh, A.; Heston, W.D. Tumor target prostate specific membrane antigen (PSMA) and its regulation in prostate cancer. *J. Cell. Biochem.,* **2004**, *91*(3), 528-539. [http://dx.doi.org/10.1002/jcb.10661] [PMID: 14755683]

[17] Gourni, E.; Henriksen, G. Metal-Based PSMA Radioligands. *Molecules,* **2017**, *22*(4)E523 [http://dx.doi.org/10.3390/molecules22040523] [PMID: 28338640]

[18] Davis, M.I.; Bennett, M.J.; Thomas, L.M.; Bjorkman, P.J. Crystal structure of prostate-specific membrane antigen, a tumor marker and peptidase. *Proc. Natl. Acad. Sci. USA,* **2005**, *102*(17), 5981-5986. [http://dx.doi.org/10.1073/pnas.0502101102] [PMID: 15837926]

[19] Horoszewicz, J.S.; Kawinski, E.; Murphy, G.P. Monoclonal antibodies to a new antigenic marker in epithelial prostatic cells and serum of prostatic cancer patients. *Anticancer Res.,* **1987**, *7*(5B), 927-935. [PMID: 2449118]

[20] Murphy, G.P. Radioscintiscanning of Prostate Cancer. *Cancer,* **1995**, *75*(S7), 1819-1822.

[http://dx.doi.org/10.1002/1097-0142(19950401)75:7+<1819::AID-CNCR2820751611>3.0.CO;2-U]

[21] Bander, N.H.; Trabulsi, E.J.; Kostakoglu, L.; Yao, D.; Vallabhajosula, S.; Smith-Jones, P.; Joyce, M.A.; Milowsky, M.; Nanus, D.M.; Goldsmith, S.J. Targeting metastatic prostate cancer with radiolabeled monoclonal antibody J591 to the extracellular domain of prostate specific membrane antigen. *J. Urol.,* **2003**, *170*(5), 1717-1721.
[http://dx.doi.org/10.1097/01.ju.0000091655.77601.0c] [PMID: 14532761]

[22] Milowsky, M.I.; Nanus, D.M.; Kostakoglu, L.; Vallabhajosula, S.; Goldsmith, S.J.; Bander, N.H. Phase I trial of yttrium-90-labeled anti-prostate-specific membrane antigen monoclonal antibody J591 for androgen-independent prostate cancer. *J. Clin. Oncol.,* **2004**, *22*(13), 2522-2531.
[http://dx.doi.org/10.1200/JCO.2004.09.154] [PMID: 15173215]

[23] Tagawa, S.T.; Vallabhajosula, S.; Jhanwar, Y.; Ballman, K.V.; Hackett, A.; Emmerich, L.; Babich, J.; Sartor, A.O.; Harshman, L.C.; Beltran, H.; Molina, A.M.; Nanus, D.M.; Bander, N.H. Phase I dose-escalation study of ^{225}Ac-J591 for progressive metastatic castration resistant prostate cancer (mCRPC). *J. Clin. Oncol.,* **2018**, *36*(Suppl. 6), TPS399-TPS399.
[http://dx.doi.org/10.1200/JCO.2018.36.6_suppl.TPS399]

[24] Vallabhajosula, S.; Kuji, I.; Hamacher, K.A.; Konishi, S.; Kostakoglu, L.; Kothari, P.A.; Milowski, M.I.; Nanus, D.M.; Bander, N.H.; Goldsmith, S.J. Pharmacokinetics and biodistribution of ^{111}In- and ^{177}Lu-labeled J591 antibody specific for prostate-specific membrane antigen: prediction of ^{90}Y-J591 radiation dosimetry based on ^{111}In or ^{177}Lu? *J. Nucl. Med.,* **2005**, *46*(4), 634-641.
[PMID: 15809486]

[25] Foss, C.A.; Mease, R.C.; Fan, H.; Wang, Y.; Ravert, H.T.; Dannals, R.F.; Olszewski, R.T.; Heston, W.D.; Kozikowski, A.P.; Pomper, M.G. Radiolabeled small-molecule ligands for prostate-specific membrane antigen: *in vivo* imaging in experimental models of prostate cancer. *Clin. Cancer Res.,* **2005**, *11*(11), 4022-4028.
[http://dx.doi.org/10.1158/1078-0432.CCR-04-2690] [PMID: 15930336]

[26] Kularatne, S.A.; Zhou, Z.; Yang, J.; Post, C.B.; Low, P.S. Design, synthesis, and preclinical evaluation of prostate-specific membrane antigen targeted (^{99m})Tc-radioimaging agents. *Mol. Pharm.,* **2009**, *6*(3), 790-800.
[http://dx.doi.org/10.1021/mp9000712] [PMID: 19361232]

[27] Cimadamore, A.; Cheng, M.; Santoni, M.; Lopez-Beltran, A.; Battelli, N.; Massari, F.; Galosi, A.B.; Scarpelli, M.; Montironi, R. New Prostate Cancer Targets for Diagnosis, Imaging, and Therapy: Focus on Prostate-Specific Membrane Antigen. *Front. Oncol.,* **2018**, *8*, 653.
[http://dx.doi.org/10.3389/fonc.2018.00653] [PMID: 30622933]

[28] Pandit-Taskar, N.; O'Donoghue, J.A.; Ruan, S.; Lyashchenko, S.K.; Carrasquillo, J.A.; Heller, G.; Martinez, D.F.; Cheal, S.M.; Lewis, J.S.; Fleisher, M.; Keppler, J.S.; Reiter, R.E.; Wu, A.M.; Weber, W.A.; Scher, H.I.; Larson, S.M.; Morris, M.J. First-in-Human Imaging with ^{89}Zr-Df-IAB2M Anti-PSMA Minibody in Patients with Metastatic Prostate Cancer: Pharmacokinetics, Biodistribution, Dosimetry, and Lesion Uptake. *J. Nucl. Med.,* **2016**, *57*(12), 1858-1864.
[http://dx.doi.org/10.2967/jnumed.116.176206] [PMID: 27516450]

[29] Evazalipour, M.; D'Huyvetter, M.; Tehrani, B.S.; Abolhassani, M.; Omidfar, K.; Abdoli, S.; Arezumand, R.; Morovvati, H.; Lahoutte, T.; Muyldermans, S.; Devoogdt, N. Generation and characterization of nanobodies targeting PSMA for molecular imaging of prostate cancer. *Contrast Media Mol. Imaging,* **2014**, *9*(3), 211-220.
[http://dx.doi.org/10.1002/cmmi.1558] [PMID: 24700748]

[30] Lakhin, A.V.; Tarantul, V.Z.; Gening, L.V. Aptamers: problems, solutions and prospects. *Acta Naturae,* **2013**, *5*(4), 34-43.
[PMID: 24455181]

[31] Hicke, B.J.; Stephens, A.W.; Gould, T.; Chang, Y.F.; Lynott, C.K.; Heil, J.; Borkowski, S.; Hilger, C.S.; Cook, G.; Warren, S.; Schmidt, P.G. Tumor targeting by an aptamer. *J. Nucl. Med.,* **2006**, *47*(4), 668-678.
[PMID: 16595502]

[32] Lupold, S.E.; Hicke, B.J.; Lin, Y.; Coffey, D.S. Identification and characterization of nuclease-stabilized RNA molecules that bind human prostate cancer cells via the prostate-specific membrane antigen. *Cancer Res.,* **2002**, *62*(14), 4029-4033.
[PMID: 12124337]

[33] Pavlícek, J.; Ptácek, J.; Barinka, C. Glutamate carboxypeptidase II: an overview of structural studies and their importance for structure-based drug design and deciphering the reaction mechanism of the enzyme. *Curr. Med. Chem.,* **2012**, *19*(9), 1300-1309.
[http://dx.doi.org/10.2174/092986712799462667] [PMID: 22304708]

[34] Barinka, C.; Byun, Y.; Dusich, C.L.; Banerjee, S.R.; Chen, Y.; Castanares, M.; Kozikowski, A.P.; Mease, R.C.; Pomper, M.G.; Lubkowski, J. Interactions between human glutamate carboxypeptidase II and urea-based inhibitors: structural characterization. *J. Med. Chem.,* **2008**, *51*(24), 7737-7743.
[http://dx.doi.org/10.1021/jm800765e] [PMID: 19053759]

[35] Novakova, Z.; Cerny, J.; Choy, C.J.; Nedrow, J.R.; Choi, J.K.; Lubkowski, J.; Berkman, C.E.; Barinka, C. Design of composite inhibitors targeting glutamate carboxypeptidase II: the importance of effector functionalities. *FEBS J.,* **2016**, *283*(1), 130-143.
[http://dx.doi.org/10.1111/febs.13557] [PMID: 26460595]

[36] Kopka, K.; Benešová, M.; Bařinka, C.; Haberkorn, U.; Babich, J. Glu-Ureido-Based Inhibitors of Prostate-Specific Membrane Antigen: Lessons Learned During the Development of a Novel Class of Low-Molecular-Weight Theranostic Radiotracers. *J. Nucl. Med.,* **2017**, *58*(Suppl. 2), 17S-26S.
[http://dx.doi.org/10.2967/jnumed.116.186775] [PMID: 28864607]

[37] Jackson, P.F.; Cole, D.C.; Slusher, B.S.; Stetz, S.L.; Ross, L.E.; Donzanti, B.A.; Trainor, D.A. Design, synthesis, and biological activity of a potent inhibitor of the neuropeptidase N-acetylated alpha-linked acidic dipeptidase. *J. Med. Chem.,* **1996**, *39*(2), 619-622.
[http://dx.doi.org/10.1021/jm950801q] [PMID: 8558536]

[38] Majer, P.; Jackson, P.F.; Delahanty, G.; Grella, B.S.; Ko, Y.S.; Li, W.; Liu, Q.; Maclin, K.M.; Poláková, J.; Shaffer, K.A.; Stoermer, D.; Vitharana, D.; Wang, E.Y.; Zakrzewski, A.; Rojas, C.; Slusher, B.S.; Wozniak, K.M.; Burak, E.; Limsakun, T.; Tsukamoto, T. Synthesis and biological evaluation of thiol-based inhibitors of glutamate carboxypeptidase II: discovery of an orally active GCP II inhibitor. *J. Med. Chem.,* **2003**, *46*(10), 1989-1996.
[http://dx.doi.org/10.1021/jm020515w] [PMID: 12723961]

[39] Jackson, P.F.; Tays, K.L.; Maclin, K.M.; Ko, Y.S.; Li, W.; Vitharana, D.; Tsukamoto, T.; Stoermer, D.; Lu, X.C.; Wozniak, K.; Slusher, B.S. Design and pharmacological activity of phosphinic acid based NAALADase inhibitors. *J. Med. Chem.,* **2001**, *44*(24), 4170-4175.
[http://dx.doi.org/10.1021/jm0001774] [PMID: 11708918]

[40] Wu, L.Y.; Anderson, M.O.; Toriyabe, Y.; Maung, J.; Campbell, T.Y.; Tajon, C.; Kazak, M.; Moser, J.; Berkman, C.E. The molecular pruning of a phosphoramidate peptidomimetic inhibitor of prostate-specific membrane antigen. *Bioorg. Med. Chem.,* **2007**, *15*(23), 7434-7443.
[http://dx.doi.org/10.1016/j.bmc.2007.07.028] [PMID: 17869524]

[41] Liu, T.; Toriyabe, Y.; Kazak, M.; Berkman, C.E. Pseudoirreversible inhibition of prostate-specific membrane antigen by phosphoramidate peptidomimetics. *Biochemistry,* **2008**, *47*(48), 12658-12660.
[http://dx.doi.org/10.1021/bi801883v] [PMID: 18983168]

[42] Ganguly, T.; Dannoon, S.; Hopkins, M.R.; Murphy, S.; Cahaya, H.; Blecha, J.E.; Jivan, S.; Drake, C.R.; Barinka, C.; Jones, E.F.; VanBrocklin, H.F.; Berkman, C.E. A high-affinity [(^{18})F]-labeled phosphoramidate peptidomimetic PSMA-targeted inhibitor for PET imaging of prostate cancer. *Nucl. Med. Biol.,* **2015**, *42*(10), 780-787.
[http://dx.doi.org/10.1016/j.nucmedbio.2015.06.003] [PMID: 26169882]

[43] Dannoon, S.; Ganguly, T.; Cahaya, H.; Geruntho, J.J.; Galliher, M.S.; Beyer, S.K.; Choy, C.J.; Hopkins, M.R.; Regan, M.; Blecha, J.E.; Skultetyova, L.; Drake, C.R.; Jivan, S.; Barinka, C.; Jones, E.F.; Berkman, C.E.; VanBrocklin, H.F. Structure-Activity Relationship of (^{18})F-Labeled Phosphoramidate Peptidomimetic Prostate-Specific Membrane Antigen (PSMA)-Targeted Inhibitor Analogues for PET Imaging of Prostate Cancer. *J. Med. Chem.,* **2016**, *59*(12), 5684-5694.
[http://dx.doi.org/10.1021/acs.jmedchem.5b01850] [PMID: 27228467]

[44] Lapi, S.E.; Wahnishe, H.; Pham, D.; Wu, L.Y.; Nedrow-Byers, J.R.; Liu, T.; Vejdani, K.; VanBrocklin, H.F.; Berkman, C.E.; Jones, E.F. Assessment of an ^{18}F-labeled phosphoramidate peptidomimetic as a new prostate-specific membrane antigen-targeted

imaging agent for prostate cancer. *J. Nucl. Med.,* **2009**, *50*(12), 2042-2048.
[http://dx.doi.org/10.2967/jnumed.109.066589] [PMID: 19910433]

[45] Nedrow-Byers, J.R.; Jabbes, M.; Jewett, C.; Ganguly, T.; He, H.; Liu, T.; Benny, P.; Bryan, J.N.; Berkman, C.E. A phosphoramidate-based prostate-specific membrane antigen-targeted SPECT agent. *Prostate,* **2012**, *72*(8), 904-912.
[http://dx.doi.org/10.1002/pros.21493] [PMID: 22670265]

[46] Behr, S.C.; Aggarwal, R.; Van Brocklin, H.F.; Flavell, R.R.; Geo, K.; Small, E.J.; Blecha, J.; Jivan, S.; Hope, T.A.; Simko, J.P. Kurhanewicz, J.; Noworolski, S. M.; Korn, N. J.; De Los Santos, R.; Cooperberg, M. R.; Carroll, P. R.; Nguyen, H.; Greene, K. L.; Langton-Webster, B.; Berkman, C. E.; Seo, Y. First-in-human phase 1 PET study of CTT1057, a novel ^{18}F-labeled imaging agent targeting prostate specific membrane antigen (PSMA) in prostate cancer. *J. Clin. Oncol.,* **2017**, *35*(15)

[47] Kozikowski, A.P.; Nan, F.; Conti, P.; Zhang, J.; Ramadan, E.; Bzdega, T.; Wroblewska, B.; Neale, J.H.; Pshenichkin, S.; Wroblewski, J.T. Design of remarkably simple, yet potent urea-based inhibitors of glutamate carboxypeptidase II (NAALADase). *J. Med. Chem.,* **2001**, *44*(3), 298-301.
[http://dx.doi.org/10.1021/jm000406m] [PMID: 11462970]

[48] Maresca, K.P.; Hillier, S.M.; Femia, F.J.; Keith, D.; Barone, C.; Joyal, J.L.; Zimmerman, C.N.; Kozikowski, A.P.; Barrett, J.A.; Eckelman, W.C.; Babich, J.W. A series of halogenated heterodimeric inhibitors of prostate specific membrane antigen (PSMA) as radiolabeled probes for targeting prostate cancer. *J. Med. Chem.,* **2009**, *52*(2), 347-357.
[http://dx.doi.org/10.1021/jm800994j] [PMID: 19111054]

[49] Rowe, S.P.; Gage, K.L.; Faraj, S.F.; Macura, K.J.; Cornish, T.C.; Gonzalez-Roibon, N.; Guner, G.; Munari, E.; Partin, A.W.; Pavlovich, C.P.; Han, M.; Carter, H.B.; Bivalacqua, T.J.; Blackford, A.; Holt, D.; Dannals, R.F.; Netto, G.J.; Lodge, M.A.; Mease, R.C.; Pomper, M.G.; Cho, S.Y. ^{18}F-DCFBC PET/CT for PSMA-Based Detection and Characterization of Primary Prostate Cancer. *J. Nucl. Med.,* **2015**, *56*(7), 1003-1010.
[http://dx.doi.org/10.2967/jnumed.115.154336] [PMID: 26069305]

[50] Chen, Y.; Pullambhatla, M.; Foss, C.A.; Byun, Y.; Nimmagadda, S.; Senthamizhchelvan, S.; Sgouros, G.; Mease, R.C.; Pomper, M.G. 2-(3-1-Carboxy-5-[(6-[18F]fluoro-pyridine-3-carbonyl)-amino]-pentyl-ureido)-pentanedioic acid, [18F]DCFPyL, a PSMA-based PET imaging agent for prostate cancer. *Clin. Cancer Res.,* **2011**, *17*(24), 7645-7653.
[http://dx.doi.org/10.1158/1078-0432.CCR-11-1357] [PMID: 22042970]

[51] Szabo, Z.; Mena, E.; Rowe, S.P.; Plyku, D.; Nidal, R.; Eisenberger, M.A.; Antonarakis, E.S.; Fan, H.; Dannals, R.F.; Chen, Y.; Mease, R.C.; Vranesic, M.; Bhatnagar, A.; Sgouros, G.; Cho, S.Y.; Pomper, M.G. Initial Evaluation of [(^{18})F]DCFPyL for Prostate-Specific Membrane Antigen (PSMA)-Targeted PET Imaging of Prostate Cancer. *Mol. Imaging Biol.,* **2015**, *17*(4), 565-574.
[http://dx.doi.org/10.1007/s11307-015-0850-8] [PMID: 25896814]

[52] Cho, S.Y.; Gage, K.L.; Mease, R.C.; Senthamizhchelvan, S.; Holt, D.P.; Jeffrey-Kwanisai, A.; Endres, C.J.; Dannals, R.F.; Sgouros, G.; Lodge, M.; Eisenberger, M.A.; Rodriguez, R.; Carducci, M.A.; Rojas, C.; Slusher, B.S.; Kozikowski, A.P.; Pomper, M.G. Biodistribution, tumor detection, and radiation dosimetry of ^{18}F-DCFBC, a low-molecular-weight inhibitor of prostate-specific membrane antigen, in patients with metastatic prostate cancer. *J. Nucl. Med.,* **2012**, *53*(12), 1883-1891.
[http://dx.doi.org/10.2967/jnumed.112.104661] [PMID: 23203246]

[53] Rowe, S.P.; Macura, K.J.; Ciarallo, A.; Mena, E.; Blackford, A.; Nadal, R.; Antonarakis, E.S.; Eisenberger, M.A.; Carducci, M.A.; Ross, A.E.; Kantoff, P.W.; Holt, D.P.; Dannals, R.F.; Mease, R.C.; Pomper, M.G.; Cho, S.Y. Comparison of Prostate-Specific Membrane Antigen-Based ^{18}F-DCFBC PET/CT to Conventional Imaging Modalities for Detection of Hormone-Naïve and Castration-Resistant Metastatic Prostate Cancer. *J. Nucl. Med.,* **2016**, *57*(1), 46-53.
[http://dx.doi.org/10.2967/jnumed.115.163782] [PMID: 26493203]

[54] Giesel, F.L.; Cardinale, J.; Schäfer, M.; Neels, O.; Benešová, M.; Mier, W.; Haberkorn, U.; Kopka, K.; Kratochwil, C. (^{18})F-Labelled PSMA-1007 shows similarity in structure, biodistribution and tumour uptake to the theragnostic compound PSMA-617. *Eur. J. Nucl. Med. Mol. Imaging,* **2016**, *43*(10), 1929-1930.
[http://dx.doi.org/10.1007/s00259-016-3447-9] [PMID: 27342416]

[55] Cardinale, J.; Schäfer, M.; Benešová, M.; Bauder-Wüst, U.; Leotta, K.; Eder, M.; Neels, O.C.; Haberkorn, U.; Giesel, F.L.; Kopka, K. Preclinical Evaluation of ^{18}F-PSMA-1007, a New Prostate-Specific Membrane Antigen Ligand for Prostate Cancer Imaging. *J. Nucl. Med.,* **2017**, *58*(3), 425-431.
[http://dx.doi.org/10.2967/jnumed.116.181768] [PMID: 27789722]

[56] Giesel, F.L.; Hadaschik, B.; Cardinale, J.; Radtke, J.; Vinsensia, M.; Lehnert, W.; Kesch, C.; Tolstov, Y.; Singer, S.; Grabe, N.; Duensing, S.; Schäfer, M.; Neels, O.C.; Mier, W.; Haberkorn, U.; Kopka, K.; Kratochwil, C. F-18 labelled PSMA-1007: biodistribution, radiation dosimetry and histopathological validation of tumor lesions in prostate cancer patients. *Eur. J. Nucl. Med. Mol. Imaging,* **2017**, *44*(4), 678-688.
[http://dx.doi.org/10.1007/s00259-016-3573-4] [PMID: 27889802]

[57] Rahbar, K.; Weckesser, M.; Ahmadzadehfar, H.; Schäfers, M.; Stegger, L.; Bögemann, M. Advantage of ^{18}F-PSMA-1007 over ^{68}Ga-PSMA-11 PET imaging for differentiation of local recurrence vs. urinary tracer excretion. *Eur. J. Nucl. Med. Mol. Imaging,* **2018**, *45*(6), 1076-1077.
[http://dx.doi.org/10.1007/s00259-018-3952-0] [PMID: 29445927]

[58] Giesel, F.L.; Will, L.; Kesch, C.; Freitag, M.; Kremer, C.; Merkle, J.; Neels, O.C.; Cardinale, J.; Hadaschik, B.; Hohenfellner, M.; Kopka, K.; Haberkorn, U.; Kratochwil, C. Biochemical Recurrence of Prostate Cancer: Initial Results with [^{18}F]PSMA-1007 PET/CT. *J. Nucl. Med.,* **2018**, *59*(4), 632-635.
[http://dx.doi.org/10.2967/jnumed.117.196329] [PMID: 29419475]

[59] Rahbar, K.; Afshar-Oromieh, A.; Seifert, R.; Wagner, S.; Schäfers, M.; Bögemann, M.; Weckesser, M. Diagnostic performance of ^{18}F-PSMA-1007 PET/CT in patients with biochemical recurrent prostate cancer. *Eur. J. Nucl. Med. Mol. Imaging,* **2018**, *45*(12), 2055-2061.
[http://dx.doi.org/10.1007/s00259-018-4089-x] [PMID: 30027419]

[60] Barrett, J.A.; Coleman, R.E.; Goldsmith, S.J.; Vallabhajosula, S.; Petry, N.A.; Cho, S.; Armor, T.; Stubbs, J.B.; Maresca, K.P.; Stabin, M.G.; Joyal, J.L.; Eckelman, W.C.; Babich, J.W. First-in-man evaluation of 2 high-affinity PSMA-avid small molecules for imaging prostate cancer. *J. Nucl. Med.,* **2013**, *54*(3), 380-387.
[http://dx.doi.org/10.2967/jnumed.112.111203] [PMID: 23303962]

[61] Banerjee, S.R.; Foss, C.A.; Castanares, M.; Mease, R.C.; Byun, Y.; Fox, J.J.; Hilton, J.; Lupold, S.E.; Kozikowski, A.P.; Pomper, M.G. Synthesis and evaluation of technetium-99m- and rhenium-labeled inhibitors of the prostate-specific membrane antigen (PSMA). *J. Med. Chem.,* **2008**, *51*(15), 4504-4517.
[http://dx.doi.org/10.1021/jm800111u] [PMID: 18637669]

[62] Banerjee, S.R.; Maresca, K.P.; Francesconi, L.; Valliant, J.; Babich, J.W.; Zubieta, J. New directions in the coordination chemistry of ^{99m}Tc: a reflection on technetium core structures and a strategy for new chelate design. *Nucl. Med. Biol.,* **2005**, *32*(1), 1-20.
[http://dx.doi.org/10.1016/j.nucmedbio.2004.09.001] [PMID: 15691657]

[63] Ray Banerjee, S.; Pullambhatla, M.; Foss, C.A.; Falk, A.; Byun, Y.; Nimmagadda, S.; Mease, R.C.; Pomper, M.G. Effect of chelators on the pharmacokinetics of ($^{99m)}$Tc-labeled imaging agents for the prostate-specific membrane antigen (PSMA). *J. Med. Chem.,* **2013**, *56*(15), 6108-6121.
[http://dx.doi.org/10.1021/jm400823w] [PMID: 23799782]

[64] Hillier, S.M.; Maresca, K.P.; Lu, G.; Merkin, R.D.; Marquis, J.C.; Zimmerman, C.N.; Eckelman, W.C.; Joyal, J.L.; Babich, J.W. ^{99m}Tc-labeled small-molecule inhibitors of prostate-specific membrane antigen for molecular imaging of prostate cancer. *J. Nucl. Med.,* **2013**, *54*(8), 1369-1376.
[http://dx.doi.org/10.2967/jnumed.112.116624] [PMID: 23733925]

[65] Banerjee, S.R.; Pullambhatla, M.; Byun, Y.; Nimmagadda, S.; Green, G.; Fox, J.J.; Horti, A.; Mease, R.C.; Pomper, M.G. ^{68}Ga-labeled inhibitors of prostate-specific membrane antigen (PSMA) for imaging prostate cancer. *J. Med. Chem.,* **2010**, *53*(14), 5333-5341.
[http://dx.doi.org/10.1021/jm100623e] [PMID: 20568777]

[66] Kilian, K. ^{68}Ga-DOTA and analogs: Current status and future perspectives. *Rep. Pract. Oncol. Radiother.,* **2014**, *19*(Suppl.), S13-S21.
[http://dx.doi.org/10.1016/j.rpor.2014.04.016] [PMID: 28443194]

[67] Eder, M.; Schäfer, M.; Bauder-Wüst, U.; Hull, W.E.; Wängler, C.; Mier, W.; Haberkorn, U.; Eisenhut, M. ^{68}Ga-complex lipophilicity

and the targeting property of a urea-based PSMA inhibitor for PET imaging. *Bioconjug. Chem.,* **2012**, *23*(4), 688-697. [http://dx.doi.org/10.1021/bc200279b] [PMID: 22369515]

[68] Benešová, M.; Schäfer, M.; Bauder-Wüst, U.; Afshar-Oromieh, A.; Kratochwil, C.; Mier, W.; Haberkorn, U.; Kopka, K.; Eder, M. Preclinical Evaluation of a Tailor-Made DOTA-Conjugated PSMA Inhibitor with Optimized Linker Moiety for Imaging and Endoradiotherapy of Prostate Cancer. *J. Nucl. Med.,* **2015**, *56*(6), 914-920. [http://dx.doi.org/10.2967/jnumed.114.147413] [PMID: 25883127]

[69] Ahmadzadehfar, H.; Rahbar, K.; Kürpig, S.; Bögemann, M.; Claesener, M.; Eppard, E.; Gärtner, F.; Rogenhofer, S.; Schäfers, M.; Essler, M. Early side effects and first results of radioligand therapy with (^{177})Lu-DKFZ-617 PSMA of castrate-resistant metastatic prostate cancer: a two-centre study. *EJNMMI Res.,* **2015**, *5*(1), 114. [http://dx.doi.org/10.1186/s13550-015-0114-2] [PMID: 26099227]

[70] Rahbar, K.; Schmidt, M.; Heinzel, A.; Eppard, E.; Bode, A.; Yordanova, A.; Claesener, M.; Ahmadzadehfar, H. Response and Tolerability of a Single Dose of ^{177}Lu-PSMA-617 in Patients with Metastatic Castration-Resistant Prostate Cancer: A Multicenter Retrospective Analysis. *J. Nucl. Med.,* **2016**, *57*(9), 1334-1338. [http://dx.doi.org/10.2967/jnumed.116.173757] [PMID: 27056618]

[71] Hofman, M.S.; Violet, J.; Hicks, R.J.; Ferdinandus, J.; Thang, S.P.; Akhurst, T.; Iravani, A.; Kong, G.; Ravi Kumar, A.; Murphy, D.G.; Eu, P.; Jackson, P.; Scalzo, M.; Williams, S.G.; Sandhu, S. [^{177}Lu]-PSMA-617 radionuclide treatment in patients with metastatic castration-resistant prostate cancer (LuPSMA trial): a single-centre, single-arm, phase 2 study. *Lancet Oncol.,* **2018**, *19*(6), 825-833. [http://dx.doi.org/10.1016/S1470-2045(18)30198-0] [PMID: 29752180]

[72] Rahbar, K.; Ahmadzadehfar, H.; Kratochwil, C.; Haberkorn, U.; Schäfers, M.; Essler, M.; Baum, R.P.; Kulkarni, H.R.; Schmidt, M.; Drzezga, A.; Bartenstein, P.; Pfestroff, A.; Luster, M.; Lützen, U.; Marx, M.; Prasad, V.; Brenner, W.; Heinzel, A.; Mottaghy, F.M.; Ruf, J.; Meyer, P.T.; Heuschkel, M.; Eveslage, M.; Bögemann, M.; Fendler, W.P.; Krause, B.J. German Multicenter Study Investigating ^{177}Lu-PSMA-617 Radioligand Therapy in Advanced Prostate Cancer Patients. *J. Nucl. Med.,* **2017**, *58*(1), 85-90. [http://dx.doi.org/10.2967/jnumed.116.183194] [PMID: 27765862]

[73] Weineisen, M.; Simecek, J.; Schottelius, M.; Schwaiger, M.; Wester, H.J. Synthesis and preclinical evaluation of DOTAGA-conjugated PSMA ligands for functional imaging and endoradiotherapy of prostate cancer. *EJNMMI Res.,* **2014**, *4*(1), 63. [http://dx.doi.org/10.1186/s13550-014-0063-1] [PMID: 26116124]

[74] Weineisen, M.; Schottelius, M.; Simecek, J.; Baum, R.P.; Yildiz, A.; Beykan, S.; Kulkarni, H.R.; Lassmann, M.; Klette, I.; Eiber, M.; Schwaiger, M.; Wester, H.J. ^{68}Ga- and ^{177}Lu-Labeled PSMA I&T: Optimization of a PSMA-Targeted Theranostic Concept and First Proof-of-Concept Human Studies. *J. Nucl. Med.,* **2015**, *56*(8), 1169-1176. [http://dx.doi.org/10.2967/jnumed.115.158550] [PMID: 26089548]

[75] McCarthy, M.; Langton, T.; Kumar, D.; Campbell, A. Comparison of PSMA-HBED and PSMA-I&T as diagnostic agents in prostate carcinoma. *Eur. J. Nucl. Med. Mol. Imaging,* **2017**, *44*(9), 1455-1462. [http://dx.doi.org/10.1007/s00259-017-3699-z] [PMID: 28474140]

[76] Schmuck, S.; Mamach, M.; Wilke, F.; von Klot, C.A.; Henkenberens, C.; Thackeray, J.T.; Sohns, J.M.; Geworski, L.; Ross, T.L.; Wester, H.J.; Christiansen, H.; Bengel, F.M.; Derlin, T. Multiple Time-Point ^{68}Ga-PSMA I&T PET/CT for Characterization of Primary Prostate Cancer: Value of Early Dynamic and Delayed Imaging. *Clin. Nucl. Med.,* **2017**, *42*(6), e286-e293. [http://dx.doi.org/10.1097/RLU.0000000000001589] [PMID: 28221194]

[77] Schmuck, S.; Nordlohne, S.; von Klot, C.A.; Henkenberens, C.; Sohns, J.M.; Christiansen, H.; Wester, H.J.; Ross, T.L.; Bengel, F.M.; Derlin, T. Comparison of standard and delayed imaging to improve the detection rate of [^{68}Ga]PSMA I&T PET/CT in patients with biochemical recurrence or prostate-specific antigen persistence after primary therapy for prostate cancer. *Eur. J. Nucl. Med. Mol. Imaging,* **2017**, *44*(6), 960-968. [http://dx.doi.org/10.1007/s00259-017-3669-5] [PMID: 28280856]

[78] Berliner, C.; Tienken, M.; Frenzel, T.; Kobayashi, Y.; Helberg, A.; Kirchner, U.; Klutmann, S.; Beyersdorff, D.; Budäus, L.; Wester, H.J.; Mester, J.; Bannas, P. Detection rate of PET/CT in patients with biochemical relapse of prostate cancer using [^{68}Ga]PSMA I&T and comparison with published data of [^{68}Ga]PSMA HBED-CC. *Eur. J. Nucl. Med. Mol. Imaging,* **2017**, *44*(4), 670-677. [http://dx.doi.org/10.1007/s00259-016-3572-5] [PMID: 27896369]